Title

From nano to macro: Studying the hierarchical structure of the corneal extracellular matrix

Authors

Quantock, Andrew J
Winkler, Moritz
Parfitt, Geraint J
et al.

Publication Date

2015-04-01

DOI

10.1016/j.exer.2014.07.018

Peer reviewed

HHS Public Access

Author manuscript

Exp Eye Res. Author manuscript; available in PMC 2016 April 01.

Published in final edited form as:

Exp Eye Res. 2015 April ; 133: 81–99. doi:10.1016/j.exer.2014.07.018.

From Nano to Macro: Studying the Hierarchical Structure of the Corneal Extracellular Matrix

Andrew J. Quantock[1], **Moritz Winkler**[2], **Geraint J. Parfitt**[2], **Robert D. Young**[1], **Donald J. Brown**[2], **Craig Boote**[1], and **James V. Jester**[2]

[1]Structural Biophysics Group, Cardiff Centre for Vision Science, School of Optometry and Vision Sciences, Cardiff University, Cardiff, Wales, UK

[2]Department of Ophthalmology and Biomedical Engineering, University of California, Irvine, Irvine, California, USA

Abstract

In this review, we discuss current methods for studying ocular extracellular matrix (ECM) assembly from the 'nano' to the 'macro' levels of hierarchical organization. Since collagen is the major structural protein in the eye, providing mechanical strength and controlling ocular shape, the methods presented focus on understanding the molecular assembly of collagen at the nanometer level using x-ray scattering through to the millimeter to centimeter level using nonlinear optical (NLO) imaging of second harmonic generated (SHG) signals. Three-dimensional analysis of ECM structure is also discussed, including electron tomography, serial block face scanning electron microscopy (SBF-SEM) and digital image reconstruction. Techniques to detect non-collagenous structural components of the ECM are also presented, and these include immunoelectron microscopy and staining with cationic dyes. Together, these various approaches are providing new insights into the structural blueprint of the ocular ECM, and in particular that of the cornea, which impacts upon our current understanding of the control of corneal shape, pathogenic mechanisms underlying ectatic disorders of the cornea and the potential for corneal tissue engineering.

1. Introduction

In the vertebrate eye, the extracellular matrix (ECM) plays a fundamental role in defining tissue form and function. The ocular connective tissues serve both as a mechanically tough and protective outer layer and at the same time define the shape and transparency of the cornea necessary to form a refractive lens for focusing light back to the retina. In general, the properties of the ocular ECM are thought to be controlled by the unique spatial organization of the tissue components, which, as is the case in other connective tissues such as tendon and ligament, are predominantly proteins, glycoproteins and glycosaminoglycans/

Address Correspondence to: James V. Jester, Ph.D., 843 Health Sciences Road, Hewitt Hall, Room 2036, University of California, Irvine, Irvine, CA 92697-4390, JJester@UCI.edu.

proteoglycans. Collagen is the principal structural element of connective tissues and while the molecular and cellular events involved in collagen fibrillogenesis are well known (Zhang et al., 2005), there is a major gap in our understanding of how the ECM and its different components are structurally organized and assembled to facilitate the functional demands of such diverse tissues.

On the cellular and molecular level, small diameter collagen fibrils in connective tissues are formed by triple helical chains of collagen peptides synthesized within the cell and then secreted and self-assembled within the extracellular space. As shown for developing tendon, short (10-30 μm) collagen fibril segments are assembled by fibroblasts within specialized extracellular compartments. These segments then grow both linearly and laterally, increasing fibril thickness and length (Birk and Trelstad, 1984). Collagen fibril segment growth has been shown using knockout mice to be related, in part, to expression of leucine-rich repeat proteoglycans and glycoproteins that influence both linear and lateral fibril fusion (Chakravarti et al., 1998; Chakravarti et al., 2000; Danielson et al., 1997; Svensson et al., 1999). Elongating fibril segments also coalesce in the developing matrix to form larger fibers, which may branch and anastomose; a process that has been suggested to be controlled by cellular contacts and exertion of cytoskeletal forces within the boundaries of the specialized extracellular compartments formed by tendon fibroblasts during development.

A similar developmental program has been proposed for the cornea involving the intracellular synthesis, modification and packaging of procollagen, followed by directed fibril assembly within corneal fibroblast-organized extracellular compartments (Birk and Trelstad, 1984). More recently, filipodial extensions from keratocytes, termed keratopodia, have been identified in developing chick cornea also suggesting the cellular directed assembly of collagen fibrils and fibril bundles during development (Young et al., 2014). While cornea and tendon show distinct developmental similarities when considering collagen fibril formation, the tissues differ dramatically in both form and function with one showing parallel alignment of collagen fibers supporting uniaxial mechanical load, while the other shows a predominantly orthogonal, interwoven arrangement supporting formation of a 3-dimensional refractive lens. How these connective tissues are constructed from the same general materials to give very different structural and functional properties is unknown, and as noted by Trelstad and Birk in 1984, the story of “the weaving of the body fabric from the warp and woof of the matrix has yet to be told (Trelstad and Birk, 1984).”

As suggested by Kokott in his studies of eye structure (Kokott, 1938), insights into the mechanisms controlling corneal shape and function may be obtained by developing a blueprint of the cornea's architecture. Over the past 20-30 years, new technologies have become available that have furthered our understanding of hierarchical structures the cornea from the smallest (nano) to the largest (macro) scale. The purpose of this article is to review some of the influential imaging technologies which have been applied to the study of the ocular ECM, and describe advances in our knowledge to which they have contributed. Application and continued refinement of these (and, of course, other) technologies will lead to a better understanding of the mechanisms controlling corneal shape and function, the discovery of pathogenic mechanisms leading to refractive error and ectatic disorders, as well as help direct novel strategies for engineering more biomimetic corneal constructs.

2. X-Ray Scattering

X-ray scattering is not, in the strictest sense, an imaging modality because tissue sub-structure is not visualised in real space. Nevertheless, very useful – and importantly, quantitative -- structural information about the organisation of the ocular ECM can be obtained across a number of length scales. Also referred to as x-ray fibre diffraction, the applicability of this approach for ultrastructural investigations of the eye lies in the fact that when a beam of x-rays is shone through excised ocular tissue, diffraction patterns produced by x-rays are scattered by the main structural component of the ocular ECM, collagen. Most of the collagen in the eye exists in the form of fibrils, which are made up of approximately parallel arrays of long thin collagen molecules, arranged with quasi-hexagonal lateral packing (Hulmes and Miller, 1979). This fairly high degree of regularity in the spatial distribution of collagen molecules leads to the preferential constructive interference of scattered x-rays in certain directions. The upshot is the production of so-called diffraction maxima, the analysis of which allows researchers to gain conformational information about the collagen molecules which gave rise to the maxima in the first place. A comprehensive treatment of the theory behind x-ray fibre diffraction studies of the ocular ECM is beyond the scope of this article, and can be found elsewhere (Meek and Quantock, 2001; Meek and Boote, 2009). Suffice it to say that x-rays scattered at relatively wide-angles (i.e. in the region of 5° of arc) provide measurements of the spacing between collagen *molecules* within fibrils, which in the hydrated human cornea are separated by about 1.6nm (Meek et al, 1991). X-ray scattering is not just limited to investigations at intermolecular distances because diffraction maxima from cornea are also found at smaller angles, which arise because of the regular spacing of uniform diameter collagen *fibrils* within lamellae, an arrangement which, as noted by Maurice (1957), is required for tissue transparency. In the hydrated human cornea the average centre-to-centre separation of collagen fibrils is about 65nm (Meek et al, 1991). A schematic representation of wide-angle x-ray scattering (WAXS) and small-angle x-ray scattering (SAXS) from regularly spaced and uniform diameter collagen fibrils as would be found in the cornea is shown in Fig. 1. It is important to appreciate, at this point, that while WAXS patterns can be recorded for all collagen-rich ocular tissues, SAXS patterns are only produced by the cornea, because of insufficient structural homogeneity on the fibrillar scale in other ECMs such as the sclera.

X-ray scatter can be sub-categorised into *equatorial* (i.e. that which is scattered perpendicular to the collagen fibril axis) and *meridional* (i.e. x-rays scattered parallel to the fibrillar axis). As alluded to earlier, analysis of the equatorial portion of the SAXS pattern from cornea provides quantitative structural information about the diameter of the collagen fibrils, their spacing, and level of order, or regularity, in the mode of their packing. The meridional SAXS pattern, on the other hand, can be analysed to ascertain information about the electron density along the axis of the collagen fibrils. As well as generating robust quantitative information about collagen intermolecular arrangements, the WAXS signal can be further interrogated to yield a numerical measure of the orientation distribution of collagen fibrils as an average of the specimen thickness (Fig. 1) This can be achieved because collagen molecules are aligned near-axially within the fibrils that they make up, an approach described in more depth by Meek and Boote (2009). And a salient feature of x-ray

scattering experiments is that they are typically carried out on hydrated, excised tissue which has not undergone any chemical fixation or other such treatment. Thus, structural data is acquired which is illustrative of the tissue close to its native state. Moreover, during data collection the x-ray beam is ordinarily passed through the whole thickness of the cornea (or the whole thickness of a dissected or partially ablated portion of cornea in some experiments), so the final values obtained are highly representative averages of the tissue as a whole.

The corneal stroma is the most widely studied ocular ECM by SAXS and WAXS. Early x-ray fibre diffraction analyses of cornea were obtained using lab-based x-ray generators, and it typically took several hours to obtain usable diffraction patterns (Goodfellow et al., 1978; Worthington and Inouye, 1985). Inasmuch as that a particular strength of the x-ray diffraction approach is that the tissue can be investigated in its native hydrated state this was clearly sub-optimal, so researchers led by Gerald Elliott and Keith Meek began to use the more intense x-ray beams produced by large synchrotron radiation sources to investigate cornea. The first published study was in 1981 based on data collected at the DESY synchrotron in Germany (Meek et al., 1981). Since that time the vast majority of x-ray fibre diffraction studies of the eye have been conducted using synchrotron radiation, notably at Daresbury SRS and Diamond in the UK, ESRF in France, and SPring8 in Japan. Nowadays, synchrotron x-ray diffraction patterns can be recorded on sensitive detectors with sub-second exposure times, and collectively SAXS and WAXS have been readily exploited to allow the collection of numerical information on collagen architecture across the ocular ECM, making a number of noteworthy contributions to our current understanding of corneal and scleral development, homeostasis and disease.

2.1. X-ray Studies of Ocular Development

Studies of corneal development in the chick cornea between embryonic days 13 and 18 have utilised WAXS and shown that the intermolecular spacing does not change over this developmental interval, despite the fact that the stroma undergoes a significant compaction and increase in transparency (Coulombre and Coulombre, 1958). As development progresses over the same period, however, it became apparent that the WAXS pattern steadily lost its fourfold rotational symmetry, consistent with the view that additional collagen was being deposited in such a manner as to obscure a template of orthogonally oriented collagen that persisted from early developmental stages (Boote et al., 2003; Quantock et al., 2003a). The chick model has also been used to track postnatal structural changes in the corneal stroma, inasmuch as WAXS has shown that a preponderance of circumferentially aligned collagen fibrils, similar to that seen in humans and other mamalian species, is already present in the peripheral cornea and limbus of normal chicks by 1 month post-hatch (Boote et al., 2009). This pattern subsequently becomes considerably more pronounced during maturation (Boote et al., 2009). A similar trend was also observed in a WAXS study of mouse postnatal corneal development (Sheppard et al., 2010), in which circumferentially aligned limbal collagen was shown to be progressively reinforced between postnatal days 10 and 28. The application of WAXS in some animal disease models has also shed some light on the structural basis of biomechanical homeostasis in the healthy eye, with studies in chicks (Boote et al., 2008; Morgan et al., 2013) and mice (Quantock et al., 2003b),

pointing to the importance of a preferential circumferential alignment of a population of collagen fibrils at the limbus.

SAXS has also been used to investigate changes in collagen fibril organisation in the chick corneal ECM as it develops and becomes transparent in the week before hatch. The first experiments on developing chick cornea, conducted at the National Synchrotron Light Source, Brookhaven Laboratory, NY (Quantock et al., 1998), confirmed that a reduction in average fibril spacing did take place between embryonic day 12, when the cornea transmits only 40% of incident white light, and day 19, when light transmission has increased significantly (Coulombre and Coulombre, 1958). Developmental studies of the secondary chick corneal stroma (reviewed elsewhere in this issue by David Birk, as well as previously by Linsenmayer and associates (1998) and by Quantock and Young (2008)) indicate that collagen fibrils exist in bundles which progressively coalesce. Within bundles, however, fibrils appear to be of uniform diameter and to be regularly spaced. The SAXS pattern from developing cornea is produced by combined x-ray scatter from collagen fibrils in bundles, and for the purposes of our investigations we note that it is relatively insensitive to the fact that variously-sized collagen-free spaces, and indeed cells, exist between the bundles. A series of SAXS experiments by Siegler and Quantock (2002), led to the suggestion of a two-phase compaction of the ECM in developing chick cornea, in which as stromal compaction proceeds fluid is initially removed preferentially from the collagen-free space between fibril bundles, and only thereafter from within the fibril bundles too. Later work by Liles and colleagues (2010) included a SAXS analysis and suggested that the changing sulphation pattern of keratan sulphate glycosaminoglycans helps fine-tune the collagen fibril organisation within bundles as the chick cornea develops and becomes transparent.

2.2. X-ray Studies of Structure-Function Relationships and Homeostasis in the Mature Eye

WAXS has been used fairly extensively to study the complex microanatomy of the human cornea, sclera and corneo-scleral junction in a quantitative manner. Early qualitative observations of SAXS patterns obtained from human corneas had pointed to a preferential directionality in the organisation of collagen fibrils at the limbus, with more collagen fibrils tending to run in a circumferential direction in this region of the tissue that at other locations across the cornea and sclera (Meek et al., 1987). This was probed in more depth using WAXS and provided quantitative information which supported the existence of an excess of circumferential fibrils at the limbus, with proposed links to the change in curvature of the eye at the limbus (Newton and Meek 1998a; 1998b; Meek and Newton, 1999). It should be appreciated, however, that the x-ray data do not allow us to ascertain if this so-called annulus of collagen fibrils at the limbus consists of a single population of bending fibrils or of tangentially directed fibrils inserting from the sclera; indeed, it is likely to be a combination of both. It should also be pointed out that the width, angular spread and collagen density in the circumferential zone is not homogeneous around the limbus in an individual eye (Newton and Meek, 1998a; Boote et al., 2011), and that, importantly, left and right human eyes are structurally distinct in this regard (Boote et al., 2006).

Over the past decade or so, continued improvements in synchrotron technology and computing power have helped progress WAXS methods to enable quantitative, thickness-

averaged maps of collagen fibril orientation to be obtained from whole adult human corneas (Aghamohammadzadeh et al., 2004; Boote et al., 2006) and scleras (Pijanka et al., 2013). The conclusions, for example, from SAXS data (Meek et al., 1987; Daxer and Fratzl, 1997) that collagen fibrils in the central region of the human cornea run preferentially in superior-inferior and medial-lateral directions has been confirmed and extended by WAXS analyses (Meek and Newton, 1999; Aghamohammadzadeh et al., 2004). Moreover, recent studies have discovered that the majority of the circumferentially oriented collagen fibrils at the corneal limbus are located in the deepest one-third of the tissue (Kamma-Lorger, et al., 2010), and that the predominantly orthogonal arrangement of collagen fibrils in the centre of the cornea occurs mostly in the posterior stroma as well (Abahussin et al., 2009; Kamma-Lorger, et al., 2010). The anisotropic collagen architecture of the cornea and sclera is suspected to have a large influence on the biomechanical performance of the ocular coat, and WAXS data has proven amenable for inclusion in predictive models. In this regard, incorporation of WAXS data in finite element analyses has facilitated the simulation of anterior (Studer et al., 2010) and posterior (Coudriller et al., 2013) eye deformation under changing intraocular pressure, and has also been used in attempts to predict the cornea's response to surgical incision (Pinksy et al., 2005).

X-ray scattering has also contributed to our understanding of normal ageing processes in the human eye, with WAXS studies by Malik and co-workers (1992) and later Daxer and associates (1998), inspiring models to explain the age-related growth of corneo-scleral fibrils. These were based, in part, on the concept of a crosslink-driven expansion of collagen intermolecular spacing, which typically increases from approximately 1.74nm to 1.86nm throughout life (Malik et al., 1992). Intermolecular changes of a similar nature have been induced in vitro by glycating corneal collagen with a sugar such as fructose (Malik and Meek, 1994), and this led the authors to propose that ultrastructural changes in the corneal stroma take place at the molecular level as we age and might be linked to glycation and the subsequent formation of intermolecular crosslinks. These in vitro changes in intermolecular packing can be prevented by including certain compounds in the glycation-inducing incubation mixture --aspirin and aminoguanidine, for example (Malik and Meek, 1994) as well as some vitamins and other analgesics such as ibuprofen and paracetamol (Malik and Meek, 1996). More recently, Hayes and colleagues (2013) used WAXS to investigate the structural mechanism of corneal cross-linking by riboflavin/UVA treatment, concluding that the cross-links induced by the therapy are likely distinct from the aforementioned natural, intermolecular cross-links that accumulate in corneo-scleral tissues with age, and instead are more readily explained by the formation of cross-links at the fibril surface and in the protein network surrounding the collagen. Collagen interfibrillar spacing has also been studied in the human cornea as a function of age, and Malik and co-workers (1992), using SAXS, reported a decrease in this parameter by approximately 8% between 20 and 90 years of age, which they postulated might be related to changes in the proteoglycan composition of the corneal ECM. Collagen fibril diameter is also age-dependent in the human cornea, measuring, on average, 30.8nm in corneas from donors under 65 years of age and 32.2nm in those over 65 years of age (Daxer at al., 1998).

Experiments utilising the meridional portion of the SAXS pattern have provided information about the distribution of electron density along the fibril axis in human sclera, and this was

used to show that dermatan sulphate proteoglycans bind to collagen fibrils in the gap zone of the collagen fibril (Quantock and Meek, 1988), in line with electron microscopic observations on rabbit and human sclera (Young, 1985). In cornea, the meridional SAXS pattern has been used to measure the D-periodic repeat at 65 nm (Meek et al., 1981; Marchini et al., 1986), shorter than the 67nm in collagen fibrils from tendon (Meek et al., 1981; Orgel et al., 2000). This difference is likely to be a consequence of more molecular tilt with respect to the fibril axis in cornea as compared to tendon, or the result of extra binding of non-collagenous material in the gap region in cornea (Meek et al., 1981; Marchini et al., 1986). Analysis of the meridional SAXS patterns from corneas has also identified hydroxyproline residues in the centre of the gap region, and proposed these as the major sites at which sugars bind to collagen (Meek et al., 1981). It has also served to identify proteoglycan binding sites along the collagen fibril axis at the *c*2 and *a*3 staining bands at each gap/overlap junction and at bands *e* and *d* in the centre of the gap zone (Meek et al., 1986). Interestingly, however, the spatial association of stained proteoglycan fibrils along the axis of the collagen fibril is different in keratoconus (Fullwood et al., 1992). SAXS has also been used to provide evidence for the binding of a glycoprotein with a molecular weight of 135kD in the gap zone of bovine corneal collagen fibrils, which has a number of similarities to one of the subunits of type VI collagen (Wall et al., 1998), and to show that the axial D-period in the human cornea increases marginally with age, possibly because of a progressive reduction in the molecular tilt with respect to the fibril axis (Daxer et al., 1998). Experiments in rabbits have shown, however, that the D-period is unaltered in corneal scar tissue (Rawe et al., 1994).

The corneas of various species have been investigated by SAXS, which has revealed that mean centre-to-centre collagen interfibrillar spacings in bony fish, fin whale and dolphins are lower than 52nm, but in other mammals range from 59nm to 73nm (Gyi et al., 1988). This study was later extended to incorporate measurements of fibril diameters and intermolecular spacings using WAXS, which disclosed no significant interspecies variation in intermolecular spacing (Meek and Leonard, 1993). Interestingly, however, a correlative link between collagen fibril diameter and interfibrillar spacing was found, inasmuch as smaller fibrils were more closely spaced. The constant parameter across species, it turns out, is the collagen fibril volume fraction, which, expressed as a percentage average across species, came out at around 28% (Meek and Leonard, 1993). Put another way, this means that in any given structural “unit cell”, 28% of the volume of the corneal stroma comes from a collagen fibril or combination of fibrils and 72% is the “space” between fibrils. This analysis led to the authors to suggest that the constancy of the fibril volume fraction in corneas of different species may be linked to requirements for light transmission and may also be reflective of a fixed proportionality in the amounts of collagen and proteoglycans across species. More recently, WAXS has shown that an excess of corneal collagen is directed towards one or both sets of rectus muscles in animals with high levels of visual acuity (Hayes et al., 2007b), which the authors speculate may be linked to the frequency of eye movement and the forces generated.

SAXS experiments have also aided our understanding of the structural roles of small leucine-rich proteoglycans in corneal homeostasis. Experiments on the corneas of gene-

targeted mice lacking the core proteins for lumican (Quantock et al., 2001; Beecher et al., 2006), keratocan (Meek et al., 2003) and mimecan (Beecher et al., 2005), for example, have indicated various degrees of ECM disturbance. This is also true in the corneas of mice with abnormalities in the transcription factor, *Klf4* (Young et al., 2009), and those with mutations in GlcNAc 6-O sulfotransferase, an enzyme which is instrumental in the sulphation of keratan sulphate (Hayashida et al., 2006).

2.3. X-ray Studies of Ocular Disease and Wound Healing

X-ray scattering has been employed in the study of ocular pathology and would healing. Keratoconus is a condition in which the cornea becomes thinned and conical. But SAXS studies of corneas of advanced keratoconus corneas obtained post-operatively revealed no evidence for a closer than normal packing of collagen fibrils (Fullwood et al., 1992). The clear implication is that a loss of collagen from the central region of the cornea, rather than a compaction of fibrils, is responsible for the clinical thinning seen in this condition. This is manifestly unlike the situation in macular corneal dystrophy where the central cornea is thinner than normal (Ehlers and Bramsen, 1978; Donnenfeld et al., 1986), and where the mostly normal diameter collagen fibrils are more closely packed proportionally (Quantock et al., 1990). Keratoconus was also studied by Daxer and Fratzl (1997) who reported a disturbance of the lobed interfibrillar SAXS reflection in x-ray patterns obtained from the centres of post-operative keratoconic corneas, which pointed to a lessening of the preferential orthogonal alignment of collagen. More contemporary, quantitative investigations of keratoconus have used WAXS to map changes in collagen orientation and distribution, and this has led to a compelling model of disease progression in which the slippage of collagen lamellae in the cornea, especially the central cornea, leads to the physical manifestations of corneal thinning and protrusion (Meek et al., 2005; Hayes et al., 2007a, 2012). Similar experimental approaches have recently been applied to investigations of the posterior segment, disclosing alterations in collagen anisotropy in the peripapillary sclera associated with primary open-angle glaucoma (Pijanka et al., 2012).

As mentioned, SAXS measurements indicate that collagen fibril spacing is reduced as an average throughout the whole depth of the cornea in macular corneal dystrophy (Quantock et al., 1990), a rare inherited disorder in which progressive corneal opacification normally starts at an early age, and which is caused by mutations in the enzymatic sulphation pathway of keratan sulphate (Akama et al., 2000). Recent SAXS studies of this disease have indicated that the major reduction in collagen fibril spacing occurs in the deeper stromal layers (Palka et al., 2010), which is possibly reflective of the proposed greater importance of keratan sulphate proteoglycans in the posterior stroma of the corneas of larger animals based on its preferential synthesis owing to a restricted oxygen supply (Scott and Haigh, 1988). WAXS experiments have also been conducted on post-operative macular dystrophy corneas and have consistently documented an unusual signal, corresponding to a periodic structure of 0.46 nm, which is not seen in x-ray patterns obtained from normal human corneas (Quantock et al., 1992; 1993a; 1997a). The origin of this additional structure is not fully explained, but is suspected to reside in the aberrantly large proteoglycan molecules, or their aggregates, that result from improper proteoglycan sulphation pathways (Quantock et al., 1996; 1997b). It is not just in macular corneal dystrophy where proteoglycan abnormalities

lead to an altered ECM, and SAXS has been used to disclose ultrastructural abnormalities in the cornea in a number of the mucopolysaccharidoses (Quantock et al., 1993b; Huang et al., 1996; Rawe et al., 1997), a family of metabolic diseases caused by the absence or malfunctioning of lysosomal enzymes needed to break down glycosaminoglycans.

Experiments employing SAXS have been used to shed light on the structural disorder of the wounded corneal ECM and the subsequent tissue remodelling as healing progresses. Full-thickness, 2mm-diameter penetrating wounds in rabbits, for example, disclose small increases in the average collagen fibril diameter and spacing as the cornea heals (Rawe et al., 1994). WAXS further showed that collagen intermolecular spacing was reduced initially, but after 6-weeks returned to normal (Rawe et al., 1994). Moreover, the SAXS patterns indicated a collagen fibril matrix which was much more structurally disordered than normal (Rawe et al., 1994). Stromal ultrastructure becomes more akin to normal as healing progresses, however, even after almost 2-yrs a wholly normal arrangement of collagen fibrils was not attained in full-thickness penetrating wounds in rabbits (Rawe et al., 1994). A significant reduction in collagen interfibrillar spacing measured by SAXS has also been documented after the rabbit stroma has been treated with a single injection of hyaluronidase to “soften” the tissue prior to attempts to mould it via the application of a hard contact lens to change the eye's refractive status (Connon et al., 2000). And with relevance to refractive surgery, a series of SAXS experiments (which led to the award of The Troutman Medal at the American Academy of Ophthalmology in 2004) were instrumental in concluding that it was not the structural disorganisation of the corneal ECM which led to corneal haze after photorefractive keratectomy, but the response of the keratocytes (Connon et al. 2003a).

In vitro corneal healing models have also been utilised, and Kamma-Lorger and associates (2009a) used WAXS to study the orientation of collagen laid down in wounded bovine corneas healing in a culture medium. A wound was created by removing the central 5mm of the cornea to half stromal depth. Corneas were allowed to heal for up to two weeks, within which time the collagen adopted a radial configuration throughout the wound and in the neighbouring tissue, which may be the result of wound contraction during this very early stage following injury. The same wound healing model was also used in a SAXS study to monitor changes in interfibrillar spacing and diameter following different types of corneal injury (Kamma-Lorger et al., 2009b), with the authors reporting that stromal swelling is more rapid for trephine-wounded corneas than in stromal flaps. The results of this aligned well with the widely-held idea that the intensity of the corneal healing response depends on the type of injury, a concept further supported by a corneal debridement wound model in mice (Boote et al., 2012), in which SAXS was used to show that structural changes in the corneal ECM (and in corneal light scattering) following debridement injury critically depend upon the wound severity, and do so specifically in terms of whether or not the epithelial basement membrane is left intact.

2.4. *X-ray* Studies *of* Corneal Swelling

When the cornea swells and becomes oedematous, often as a result of corneal endothelial dysfunction, light scattering increases and vision is impaired. Hodson (1997) and Elliott and Hodson (1998) have extensively discussed how and why the cornea swells. From neutron

diffraction experiments on highly hydrated corneas it was surmised that the swollen cornea is essentially a system of mutually repelling cylinders (Elliott et al., 1982). SAXS studies have further shown that when the cornea becomes oedematous collagen fibrils do not swell along their axes; the D-period is unchanged (Huang and Meek, 1999). Rather, the tissue swells by fibrils and molecules moving apart laterally, and a linear relationship between the square of the collagen interfibrillar spacing and tissue hydration has been demonstrated (Goodfellow et al.,1978). Meek and associates (1991) subsequently confirmed this linear relationship in a series of correlative SAXS and WAXS experiments on isolated bovine corneas which were placed in dialysis membranes and variously hydrated by a range of external osmotic strength bathing solutions. These authors calculated (by extrapolation) that at zero hydration the centre-to-centre collagen fibril separation would be 34nm. But, this is less than the diameter of the hydrated fibrils in bovine cornea, which is 38nm according to Meek and Leonard (1993), so it was concluded that the fibrils themselves must reduce in diameter during drying. Collagen intermolecular spacing was found to be 1.15nm in the dry tissue and 1.60nm at physiological hydration (Meek et al., 1991). Interestingly, however, when the cornea was taken to high hydrations the intermolecular spacing increased very little above the 1.60nm value. SAXS measurements of collagen interfibrillar spacing, on the other hand, continued to increase with increasing hydration above physiologic. If corneal hydration (H) is defined as H = (wet weight – dry weight)/(dry weight), the combined SAXS and WAXS data showed that intermolecular and interfibrillar spacings increased in proportion with one another from H=0 to H=1, suggesting that, from dry, water goes equally into the fibrils and between them. Above H=1, however, and up to high hydrations the bulk of the water goes solely between the fibrils, presumably because intermolecular bonds are fully extended already when the cornea is at 50% hydration (Meek et al., 1991). This model of corneal swelling was broadly supported by subsequent x-ray diffraction studies which proposed a two-stage drying model with a transition between the two stages occurring at H=1 (i.e, 50% hydration) (Fratzl and Daxer,1993). SAXS work on overly hydrated human corneas in excess of 800 μm thick has also shown that the bulk of interfibrillar swelling occurs in the deeper stromal layers, presumably because of the higher degree of interweaving which is a feature of more anterior stromal layers (Quantock et al., 2007).

Hopefully, this selective review of x-ray scattering studies of the ocular ECM, and of the corneal matrix in particular, have provided some insights into the value of the approach and of the highly representative structural averages it can provide over a number of length scales in non-fixed, physiologically hydrated tissue. The fact that x-ray scattering is an excellent averaging tool, however, is also to its detriment because focal defects in ECM structure are below the spatial resolution of the approach. Thus, for a good overarching understanding of the ultrastructure of the ocular ECM, correlative work with techniques such as those to be described in the remainder of this article are highly valuable.

3. Electron Microscopy

Electron optical imaging has made a major contribution to studies of the ocular ECM for over sixty years. When the earliest observations on the ultrastructure of the corneal stroma were published (Jakus, 1954), the best resolution of the transmission electron microscope was still only around 300 nm, compared with under 4 Å possible in microscopes available

today. Inevitably, advances in both specimen preservation and instrumentation have driven new discoveries ever since. Several key changes in the first basic specimen processing schedules lead to much improved tissue preservation, and these are still currently in use for routine observations. Amongst these, the replacement of single-step osmium tetroxide fixation by a two-step procedure using aldehyde primary fixation (Sabatini et al., 1963), followed by osmium, allowed superior preservation of matrix and cell membranes; also, the introduction of epoxy embedding resins (Glauert et al., 1956), in place of glycol methacrylate, provided both improved ultrathin sectioning properties, and specimen stability in the electron beam. Electron microscopy rapidly found a place in investigative studies of the fine structural anatomy and of tissue changes in pathological conditions of the major connective tissue components of the eye, the cornea and sclera (Hogan et al., 1971; Polack, 1976), and trabecular meshwork (Tektas & Lütjen-Drecoll, 2009; Lütjen-Drecoll, 1999). This trend continues undiminished, but now with a more analytical focus on compositional and 3-dimensional aspects of matrix structure, following a succession of refinements in technique and instrumentation, as illustrated further below.

3.1 Collagen Organisation in the Ocular ECM

The corneal stroma has dominated ultrastructural studies of the ocular ECM largely on account of the fascination with, and desire to understand, the structural basis of the tissue's unique transparency. The comprehensive early studies of Hay (Hay and Revel, 1969; Hay 1979) on the embryonic chicken provided the baseline for our current understanding of development of the corneal stroma. This was found to appear first as a one micron thick primary stroma of layered orthogonal collagen fibrils, laid down by the epithelium. Subsequently, an innovative study by Birk and Trelstad (1984) used high voltage electron microscopy on one micron-thick sections of embryonic stroma to investigate how keratocytes formed the characteristic lamellae of the mature transparent tissue. Bundles of collagen fibrils appeared in cell membrane channels later to fuse into larger lamellar assemblies. It now appears that corneal development in other vertebrates, primates and man included, may not involve a primary stromal template and thus corneal development is still the subject of active investigation. Early studies revealed the regular size and order of component collagen fibrils in the stroma enabling Maurice (1957) to put forward his lattice theory of corneal transparency, and numerous researchers since that time have tried to understand the factors controlling fibril diameter and spacing.

The hypothesis that interfibrillar proteoglycans might control the nucleation and regulation of fibril diameter lead Borcherding and colleagues (1975) to examine fibril diameter in relation to specific proteoglycan concentrations from the central cornea to the sclera in human eyes. The relationships between high levels of keratan sulphate glycosaminoglycan and small fibril diameter in the mid cornea, translating to high chondroitin sulphate levels with larger fibril diameters towards the sclera, lent support to this theory. Corneal proteoglycans are now understood to be a heterogeneous population: keratan sulphate glycosaminoglycan chains are substituted on three main core proteins as lumican (Blochberger et al., 1992), keratocan (Corpuz et al., 1996; Liu et al., 1998) and mimecan (Funderburgh et al., 1997) proteoglycans, with minor amounts also present as fibromodulin (Chen et al., 2010); decorin core protein carries chondroitin sulphate/dermatan sulphate side

chains (Li et al., 1992). Electron microscopy has become a vital tool in assessing the regulatory roles of these molecules on the corneal collagen matrix in studies of altered fibril diameters in mice with targeted gene knockouts. Lumican-null mice, for example, expressed increased fibril diameters, altered fibril packing and disordered lamellae in the posterior stroma (Chakravarti et al., 1998; 2000); altered fibrils were also found in the sclera, where lumican is present as a glycoprotein with short unsulphated keratan sulphate chains (Austin et al., 2002). Mice deficient in keratocan and mimecan also exhibited altered collagen fibril diameters (Liu et al., 2003; Tasheva et al., 2002). The advantage of high resolution region-specific analysis offered by electron microscopy has been clearly demonstrated in several recent studies. For example, posterior stromal regions were found to be more severely affected by the disruption of fibril structure and organisation in decorin/biglycan compound mutant mice, suggesting a synergy of regulatory roles for proteoglycans, in this case decorin and biglycan, in matrix assembly (Zhang et al., 2009). As mentioned earlier, the deep stroma is also the most affected corneal region in macular corneal dystrophy, and this is where pockets of abnormally large diameter collagen fibrils are found (Palka et al., 2010). A subsequent study of the peripheral cornea in mice further showed that fibromodulin may cooperate with lumican in fibril regulation during postnatal corneal development (Chen et al., 2010).

3.2 Glycosaminoglycan Imaging with Cationic Dyes and Immunogold Probes

The poly-disperse nature of interfibrillar matrix proteoglycans and their inherently low electron contrast at first prevented successful imaging of these molecules. Attempts to bind cationic electron dense markers, such as ruthenium and lanthanum to the charged sulphate groups on glycoaminoglycans enabled limited imaging, and merely of their condensed collapsed structure. The introduction of the cationic copper dyes, cuprolinic and cupromeronic blue based on alcian blue, by Scott (1981), and their use with competing cations (the ‘critical electrolyte concentration’ technique), was a major advance, allowing visualisation of proteoglycans as extended electron dense filaments which associated at regular sites along the axial periodic banding pattern of the collagen fibril (Fig. 2). Pre-digestion of tissue with specific proteoglycan degrading enzymes conferred some specificity on the method, indicating that keratan sulphate and chondroitin sulphate/dermatan sulphate proteoglycans bound to ‘a’ and ‘c’, and ‘d’ and ‘e’ bands, respectively in the rabbit cornea (Scott et al., 1985). Sclera, in human and rabbit, exhibited ‘d’ and ‘e’ banding alone, resembling tendon (Young, 1985), later confirmed by x-ray analysis (Quantock and Meek, 1988). Although this approach still represents the optimal method for obtaining structural information on proteoglycans imaged in bulk tissue, it has to be accepted that some collapse of native structure is the sacrifice paid to induce electron contrast. Only with proteoglycan molecules isolated from the eye in suspension, and dried onto an ultra-clean surface to be examined by rotary shadowing electron microscopy have images of actual molecular dimensions been possible (Ward et al., 1987; Scott, 1996). Even with this limitation, cationic dye staining has been widely used to examine proteoglycans in ocular ECM research: for example, in the developing corneal stroma of rabbit and chick (Cintron and Covington, 1990; Connon et al., 2003b; Liles et al., 2010); in healing corneal scars (Hassell et al., 1983); changes in cornea with lysosomal storage diseases (Young et al., 2011); after

crosslinking treatment in keratoconus (Akhtar et al., 2013); and, in scleritis (Young et al., 1988).

The use of electron histochemical and immunolocalistion techniques at the ultrastructural level was revolutionized by the introduction of colloidal gold as a marker system (Faulk and Taylor, 1971). Colloidal gold particles of 1 nm diameter together with two-stage antibody procedures, in theory could allow epitope localisation with a resolution of just over 8 nm, but methods with nanogold markers exceeded this. The development of low temperature specimen processing with hydrophilic acrylate/methacrylate resins, such as Lowicryl and LR White, allowed improved preservation of protein conformation and thus better antigen efficacy by avoiding the need for complete tissue dehydraton. Together with more refined techniques for cryoultramicrotomy, studies using specific monoclonal antibodies then permitted precise identification of epitope-defined structures within ultrathin sections. Multiple epitope labelling made possible with these methods enabled Birk and co-workers (1988) to demonstrate that corneal collagen fibrils were heteropolymeric, containing both types I and V collagens in the same fibril. Subsequently, Marshall and associates (see review, 1993) carried out extensive immunogold localisation of collagen types in diverse extracellular matrices in the human eye including cornea, sclera, iris, trabecular meshwork, ciliary body and retina, reporting positive labelling for collagen type III in cornea, which remains somewhat controversial (Marshall et al., 1991). Immunogold labelling of proteins, such as collagens, is not straightforward when antibody epitopes may reside in the triple helical domain of the molecule and be modified by crosslinking with the aldehyde fixatives used in many conventional procedures for tissue preservation. Although this problem exists also for antibodies raised against the core proteins of proteoglycans, antibodies reacting with glycosaminoglycan side chains of proteoglycans retain immunoreactivity after aldehyde fixation (Fig. 3). Some of the most widely used antibodies against proteoglycan domains, such as 5-D-4 and 1-B-4, recognize different sulphation motifs present on the repeat disaccharide moieties of keratan sulphate and chondroitin sulphate proteoglycans (Caterson et al., 1983; 1985). These reagents have been used extensively in studies of glycosaminoglycan sulfation associated with matrix development and pathlogy in cornea (Davies et al., 1997; Young et al., 2006; 2007; Lewis et al., 2000), and other ocular connective tissues.

3.3 Cryo-Techniques

In the 1980s a general acceptance of the structural changes brought about by conventional tissue processing techniques for electron microscopy was replaced by new optimism with a greater awareness and availability of low temperature tissue preparation methods. Notwithstanding the known extraction and collapse of delicate hydrated tissue components such as interfibrilllar proteoglycans, an x-ray scattering study on cornea confirmed that shrinkage artefact at all stages of conventional processing schemes reduced the true structural dimensions of collagen from the molecular level, seen as a reduction in the D-period, through to the level of fibril spacing (Fullwood and Meek, 1993). Fibril diameters were 45% larger when cornea was processed at low temperature, more resembling their native dimensions recorded by low-angle x-ray diffraction (Craig et al., 1986). Ultra-rapid freezing, aiming to freeze tissue without the deleterious effects of ice crystal formation, was

considered desirable as this could potentially avoid all of the preparation-induced artefacts associated with aqueous chemical fixation. Hirsch and co-workers (2001) achieved remarkable results using the method of ultrarapid freeze and deep etch. Human and rabbit cornea were slam-frozen on a liquid helium-cooled copper block, then fractured and etched, still frozen under vacuum. A replica was made by platinum/carbon evaporation onto the surface and this was viewed in the transmission electron microscope. 8nm collagen sub-fibrils together with a range of beaded and filamentous interfibrillar structures were interpreted as proteoglycans, type VI and FACIT collagens, types XII and XIV on the basis of their dimensions. The technique has also been applied to study interactions at the cell-matrix interface in the eye, in three dimensional keratocyte cultures (Bueno et al., 2009), and in age-related changes in Bruch's membrane (Ruberti et al., 2003). Cooling rates achievable by slam freezing, however, are too slow to achieve ice-crystal-free freezing much deeper than 15 μm into bulk tissue and thus, while suitable for surface observations, this technique has limitations where larger areas are to be studied. High pressure freezing overcomes this drawback (Moor, 1987) and has been shown capable of vitrification, where ice assumes an amorphous, glassy state - in theory arresting native tissue structure - to a depth of 200 μm in articular cartilage specimens (Studer et al., 2008). Nevertheless, the clear advantages of this approach have not to date been exploited to any great extent in studies of the ocular connective tissues: highly-hydrated specimens have previously proven difficult to cryofix effectively, however cell ultrastructure and collagen fibril structure and spacing appeared well-preserved in high pressure frozen chicken embryo cornea (Allenspach, 1993; Quantock and Young, 2008; Fig. 4).

3.4 Electron Tomography and Three-Dimensional Imaging

Increasingly powerful computing capabilities and improved cameras for image recording, alongside automation of electron microscope operation have combined over the last two decades to promote electron tomographic analyses of large tilt series of images to almost a routine procedure in many laboratories. This has facilitated sophisticated studies of molecular and supramolecular organisation in connective tissues, several on the ocular matrices. Elegant work by Holmes and colleagues (2001) employing Fourier filtering of high resolution serial tilted images allowed three-dimensional reconstruction of individual isolated bovine collagen fibrils, revealing component 4 nm microfibrils with a consistent tilt angle of 15° respective to the fibril long axis. Resolution was sufficient to also visualise structures at the fibril surface, potentially proteoglycans, type V collagen N-propeptide and collagen types XII and XIV. Microfibrils in extended and untensioned states were plotted by electron tomography in fibrillin from human and bovine lens zonules to derive models predicting the respective molecular conformational alignments (Baldock et al., 2001). Three-dimensional ultrastructural studies enabled Knupp and co-workers (2000; 2002; 2006) to identify as type VI collagen, molecular assemblies with around 100 nm periodicity found in the retina of patients with age-related macular dystrophy, Sorsby's fundus dystrophy, and in the vitreous in association with macular holes. Electron tomography in combination with earlier cationic dye staining methods for proteoglycans (Fig. 5) has helped challenge some earlier ideas of corneal matrix interactions derived from two dimensional observations (Lewis et al., 2010; Parfitt et al., 2010; 2011). From previous models (Maurice, 1962; Farrell and Hart, 1969; Muller et al., 2004) a systematic six-fold arrangement of proteoglycans

associating each collagen fibril with its nearest neighbours was envisaged. In bovine (Lewis et al., 2010) and mouse stroma (Parfitt et al., 2010), no regular pattern of proteoglycan organisation was detected. Thermal motion and osmotic pressure control were proposed as mechanisms by which proteoglycans might regulate interfibrillar spacing rather than through inflexible attachments to fibrils. Keratan sulphate proteoglycans were represented by shorter dye complexes, attaching neighbouring fibrils, while chondroitin sulphate/dermatan sulphate proteoglycans were longer, probably formed from multimeric chains, and capable of linking both neighbour and 'next-nearest' neighbour fibrils. Three-dimensional reconstructions on corneas from *Chst*-5 mutant mice with defective sulphation of keratan sulphate proteoglycans revealed grossly enlarged proteoglycan structures, consistent with compensatory over-sulphated or aggregated chondroitin sulphate/dermatan sulphate proteoglycans, which span and likely interact with many more collagen fibrils than their counterparts in wild type mice (Parfitt et al., 2011).

3.5 Scanning Electron Microscopy

With the burgeoning interest in three-dimensional structural biology, a new ultrastructural imaging technique based on scanning electron microscopy (SEM) has recently emerged. Significant improvements in the resolution of scanning electron microscopes now allow the instrument to compete with the transmission microscope in its imaging performance. SEM has traditionally been a surface imaging technique and has occasionally been employed in ocular matrix research, notably in studies of cell and lamellar organisation, and repair in the cornea. Nishida and associates (1988) used tryptic digestion and acid hydrolysis to remove stromal collagen to reveal the corneal keratocytes and their interconnecting network of processes, which they proposed facilitated cellular control of corneal homeostasis and transparency. Komai and Ushiki (1991) incorporated alkali etching techniques in their processing schedule, to remove cellular and perifibrillar matrix and achieve detailed images of collagen fibril organisation in different regions of the human cornea and sclera. A later study using similar techniques revealed that the extent of cross-lamellar interweaving in human anterior corneal stroma was far greater than previously thought (Radner et al., 1998); a scanning electron microscopy study by Cintron and co-workers (1982) on corneal scarring found that new collagen deposition showed alignment with fibroblasts which, in turn oriented with respect to the healing epithelium. More recently, post-LASIK human corneas were studied revealing evidence that scar tissue at the wound interface may never restore intact lamellar integrity at this site (Abahussin et al., 2013). The revolution in approach to scanning electron microscopy relies upon the simple concept that if a high resolution image taken of the specimen surface can be alternated with the removal of a surface slice, a new surface is created for subsequent imaging. With recent advances in computerisation of instrument control, together with improved backscatter electron detectors, this process can be automated to collect a large image sequence, progressing for many μm or even mm into the specimen, such that the serial images can then be aligned, if required, and processed electronically to generate a three-dimensional rendering of structures throughout the specimen. This 'volume scanning electron microscopy' can be achieved with a dual beam instrument (Knott et al., 2008) in focused ion beam electron microscopy (FIB SEM), where a Gallium ion beam mills away a layer of the surface, before the electron beam is employed to image the newly exposed surface of the resin block. The ion beam is able to mill

thicknesses as low as 5nm, which also equates to the resolution limitation in z. Alternatively, in a single beam instrument, specimen surface renewal can be carried out by a miniature ultramicrotome situated inside the microscope chamber (Denk and Horstmann, 2004; Hughes et al., 2014) in serial block face scanning electron microscopy (SBF-SEM). In this case, 15-20 nm is currently the lower limit practicable for biological specimens. Few studies have yet been carried out on ocular tissues with these new methods. Basement membrane vacuolation in retinal capillaries was studied in normal and diseased eyes by SBF-SEM (Powner et al., 2011). Both sectioning approaches were applied to study corneal development in the chick, revealing that cellular components represent a much higher proportion of the embryonic matrix than was previously thought from two-dimensional images, probably because of the abundance of filopodial extensions from the cells (Fig. 6), which appear to fulfil a role in assembly of the prospective lamellar matrix (Bushby et al., 2011; Young et al., 2014). Volume SEM already shows huge potential for imaging three dimensional microanatomy in large tissue volumes, with resolution at the level of sub-cellular organelles, individual collagen fibrils and cell membranes. It promises to offer even greater investigative opportunities in the coming years with the recent development of novel labelling technologies, such as the genetic tags APEX (enhanced ascorbate peroxidase; Martell et al., 2012) and miniSOG (mini singlet oxygen generator; Shu et al., 2011), enabling specific electron dense markers to be expressed within bulk tissue, which will facilitate correlative studies with light microscopy and live cell imaging techniques.

4. Non-linear Optical (NLO) Imaging of Second Harmonic Generated Signals (SHG)

Non-linear optical (NLO) imaging using second harmonic generated signals (SHG) has emerged as a powerful new paradigm for three-dimensionally detecting and evaluating collagen organization. SHG is an absorption-free, nonlinear process created in non-centrosymetric materials when excited using high intensity radiation (Franken et al., 1961; Goppert-Mayer, 1931). In biologic tissues, SHG signals can be generated using long wavelength (infrared), very fast pulsed, femtosecond (FS) lasers. Due to the extremely high field strengths associated with femtosecond laser pulses, an oscillating polarization of non-centrosymetric biologic materials results in the emission of light at exactly half the wavelength of the laser excitation beam. Owing to the nature of the process it occurs only in the focal plane of the laser beam, yielding high lateral and axial resolution ($\sim 1\ \mu m$). Because SHG is limited to structures that lack central symmetry, this imaging paradigm is highly specific for longitudinally oriented, fibrillar collagen and does not require prior tissue staining, fixation or sectioning (Williams et al., 2005; Zipfel et al., 2003). Additionally, the high axial resolution allows for three-dimensional image acquisition deep into tissues and the reconstruction of tissue collagen organization not previously available through other conventional microscopic techniques.

The ability to detect SHG signals from the cornea was first demonstrated by Hochheimer in 1984 using a pulsed YAG laser (Hochheimer, 1982); however, it was not until 2002 that the first microscopic images showing collagen organization within the cornea were reported by Yeh et al using 170 FS pulsed laser (Yeh et al., 2002). Over the past decade, NLO SHG

imaging has been used to evaluate corneal collagen in normal corneas from human (Aptel et al., 2010; Han et al., 2005; Morishige et al., 2006), mouse (Lo et al., 2006), pig (Jay et al., 2008; Teng et al., 2006; Wang et al., 2008), and rabbit (Morishige et al., 2006), as well as used to study pathologic conditions, such as keratoconus (Morishige et al., 2007; Tan et al., 2006), intrastromal laser ablation (Han et al., 2004; Wang and Halbhuber, 2006), thermal injury (Lo et al., 2009; Tan et al., 2005), transgenic mouse models (Lyubovitsky et al., 2006), infectious keratitis (Tan et al., 2007), wound healing (Farid et al., 2008; Nien et al., 2011; Teng et al., 2007), corneal edema (Hsueh et al., 2009; Wu and Yeh, 2008), collagen crosslinking (Bueno et al., 2011), and diabetes (Latour et al., 2012b). More recently, objective measures have been developed to characterize collagen orientation by using fast Fourier transformation (Ghazaryan et al., 2013; Lau et al., 2012; Lo et al., 2012; Mega et al., 2012; Rao et al., 2009; Tan et al., 2013) and by taking advantage of the unique polarization dependent properties of SHG signals (Latour et al., 2012a; Stoller et al., 2002; Tuer et al., 2012).

We have used NLO SHG to evaluate collagen organization in the intact cornea of various species, including human, and confirmed and extended earlier observations regarding the interwoven nature of the collagen fiber (i.e. lamellar) architecture previously identified using transmission and scanning electron microscopy (Hamada et al., 1972; Komai and Ushiki, 1991; Muller et al., 2001; Radner et al., 1998). To begin to build a blueprint of the corneal collagen architecture, we have also developed a High Resolution Macroscopic (HRMac) approach for scanning large tissue areas (up to 1.6 cm across) at high resolution (0.44 μm/pixel) and digitally reconstructing the images as described below. This provides “Google Maps” of the cornea, in which single collagen lamellae can be followed and their structural interactions with remote collagen lamellae characterized. Using this approach we have begun to characterize the entire cornea from limbus-to-limbus and relate these structural/architectural features to localized mechanical measurements to better understand how collagen structure controls mechanical strength and corneal shape.

4.1 NLO SHG Imaging of Corneal Collagen

For these and all other studies discussed below, we have used a Zeiss LSM 510 Meta confocal microscope (Carl Zeiss Inc., Thornwood, NY) and a Chameleon Titanium:Sapphire laser (Coherent Inc., Santa Clara, CA) that produces 150 femtosecond (FS) laser pulses at 76 MHz. Since SHG signals are polarization dependent, a 1/4 wave plate was interposed between the laser and the microscope to produce circularly polarized FS laser light and ensure SHG generation from all in plane collagen fibers regardless of orientation. Optimal SHG signal generation was obtained by tuning the laser to 800 nm, which has been shown to produce the strongest signal intensity from fibrillar collagen (Zoumi et al., 2002), as well as from the cornea and optic nerve head (Morishige et al., 2006; Winkler et al., 2010b). Tissues were then mounted on the microscope stage, either fresh without fixation, or following overnight fixation in 2% paraformaldehyde in phosphate buffered saline, pH 7.2. Unlike glutaraldehyde fixation, fixation with paraformaldehyde showed no effect on SHG signal intensity and had the advantage of greatly preserving collagen orientation similar or identical to that detected in intact globes under normal intraocular pressure. Using fresh corneal tissue without fixation produced images of collagen lamellae that were severely

crimped or undulated due to the artifactual mechanical unloading of the lamellae. For this reason, studies generally used corneal tissue that was fixed in situ or imaged with the globes intact.

FS laser light was focused into the tissues using either a 20x/NA 0.8 or 40x/NA 1.2 Zeiss apochromatic objective. To detect SHG signals, a transmitted light detector with a 400/50 nm band pass filter was used to collect forward scattered SHG signals. Backscattered SHG signals were collected using the Meta detector of the Zeiss LSM microscope and a bandwidth setting of 380-420 nm. In general, forward scattered SHG signals detected distinct fiber-like structures within the cornea that were approximately 1 μm in diameter and varied in length and orientation depending on the depth within the cornea (Fig. 7, Cyan). Since collagen fibrils in the cornea are approximate 32 nm in diameter, the detected fibers most likely represent fibril bundles within the larger diameter collagen lamellae of the cornea. Backscattered SHG signals showed a more diffuse and less distinct image of the individual collagen lamellae within the cornea as shown in Fig. 7, Magenta. Data stacks were collected in 1-2 μm steps from the anterior surface of the cornea to a depth of 160 μm using the 40x objective and through the entire cornea with the 20x objective. The resolution obtained using this approach was 0.44 μm to 0.88 μm lateral and 1-2 μm axial.

4.2 Collagen Structure of the Cornea as Detected using NLO SHG

Using en face NLO SHG imaging, collagen structure can be evaluated throughout the entire thickness of the cornea as shown in Fig. 8 (Morishige et al., 2007). The first signals appear at the level of Bowman's layer, or the anterior limiting lamina (ALL), a more descriptive term outlined by the Terminologia Anatomica (Federative Committee on Anatomical Terminolgy, 1998) that will be used throughout the following text. Backscattered SHG signal show a very weak punctate forward scattered signal (A) and a stronger diffuse backscattered signal (B). Ten microns below the ALL, narrow bands of short collagen lamellae aligned in random orientations are detected (Fig. 1C) that are consistent with the narrower and thinner lamellae comprising the anterior corneal stroma observed by TEM and SEM (Komai and Ushiki, 1991; Radner et al., 1998). The backscattered SHG signal shows a less distinct, albeit clearly interwoven, pattern of collagen fibers in the same optical plane (Fig. 1D). Deeper into the cornea (50 μm) collagen fibers appeared longer and wider but continue to be oriented in random directions (Fig. 1E and F). Three-dimensional reconstruction and rotation of the data along the *Y*-axis to generate an *XZ* projections shows that many of the short collagen fibers identified in the anterior stroma by the forward scattered SHG signal represent much longer fibers running transverse to the surface, originating at ALL and penetrating deep into of the anterior stroma (Fig. 1G). Three dimensional reconstruction of the backscattered SHG signal clearly identifies the presence of the ALL (Fig. 1H, asterisk) and the multiple layered collagen lamellar organization running both parallel and transverse to the corneal surface. This organizational pattern appears remarkably similar to that of routine hematoxylin and eosin stained corneal tissue sections, but has the obvious benefit that NLO SHG imaging does not require tissue fixation, sectioning or staining to appreciate the collagen structural details.

NLO SHG imaging of other mammalian species, including mice and rabbit, shows a similar pattern of collagen lamellar organization, particularly for the presence of collagen fibers that run transverse to the ALL (Morishige et al., 2006). The presence of transverse fibers and the random orientation is distinct from the more conventional view that corneal collagen is orthogonally arranged and runs parallel to the corneal surface. However, it should be noted that angled collagen fibers were detected by polarization microscopy (Bron et al., 1997). Furthermore, the first description of angled collagen fibers was by Sir William Bowman in his monograph on parts of the eye presented at the Royal College of Surgeons of England in 1847 (Bowman, 1849). Here, Sir William notes that the presence of angled collagen fibers "might be shown on mechanical principles to be the best possible for the maintenance of the convexity of the front of the cornea".

To assess whether angled collagen fibers play a mechanical role in controlling corneal shape, we have evaluated the collagen structure of keratoconus corneas. As shown in Fig. 9, keratoconus corneal buttons obtained from penetrating keratoplasty show a distinct decrease in the number of angled collagen fibers underlying the intact ALL that are detected by forward scattered SHG (C). Additionally, less interweaving of collagen lamellae is detected by backscattered SHG (D) compared to normal. Deeper into the anterior stroma (50 μm), the loss of forward scattered SHG signal and collagen lamellae is more dramatic (E) and lamellar interweaving is completely absent (F). Three-dimensional reconstruction confirms that the number of angled collagen lamellae inserting into the ALL (asterisk) is remarkably reduced (G, arrow) and when present only extends a short distance into the anterior cornea. Reconstruction of the backscattered SHG signal also confirms the marked lack of collagen lamellar interweaving below the ALL (asterisk), showing predominantly a fiber alignment parallel to the corneal surface (H), a pattern which was distinctly different from that of normal adult cornea (Fig. 9H). In a series of 13 keraotoconus buttons, 12 cases showed severe disruption or loss of angled collagen fibers inserting into the ALL as compared to six normal corneas evaluated by NLO SHG. The one case where loss of angled fibers was not detected was in a sample that only had half of the corneal button, suggesting sampling error for this case (Morishige et al., 2007).

The loss of angled collagen lamellae in the anterior stroma of keratoconus corneas supports the hypothesis first opined by Sir William Bowman, that these structures lend mechanical support to the anterior stroma to maintain corneal shape. Loss of these mechanical "struts" would perhaps facilitate the slippage of collagen from the central cornea leading to progressive astigmatism as suggested by the x-ray scattering data discussed above (Meek et al., 2005 Hayes et al., 2007a; 2012) and by previous investigators (Polack, 1976; Smolek and Klyce, 2000). Clearly, a better understanding of how collagen lamellae are organized in normal and keratoconus corneas is needed to determine the importance of these structures to the maintenance of corneal shape and the pathogenesis of this disease.

4.3 High Resolution Macroscopy and Identifying the Corneal Collagen Architecture

To obtain data on the density and distribution of angled collagen fibers and their relationship and interactions with other corneal collagen lamellae, a larger view of the collagen organization is needed. Unfortunately, NLO SHG signal generation is a function of the

square root of the excitation power, and SHG signals are only generated in the focal volume of the FS laser beam where the laser intensity is high enough to cause non-linear processes. While this results in sub-micron lateral and axial resolution capable of resolving microstructural details of collagen lamellae, the inverse relationship between magnification and field of view means that SHG images of any given tissue only cover a very small area and even the relatively small structures that comprise the human eye are much larger in comparison to the field of view.

To address this problem, we used High Resolution Macroscopy (HRMac), which combines SHG imaging with automated image acquisition and digital image reconstruction (Winkler et al., 2010a). Using HRMac large-scale, three-dimensional image mosaics several millimeters or even centimeters across can be generated that retain the same high resolution of NLO SHG imaging. This approach enables the study of both micro- and macrostructure simultaneously by allowing the traversal of different image scales to ‘zoom’ in and out of the sample and follow single collagen lamellae. The resulting datasets can be further processed for quantitative analysis or for three-dimensional visualization and reconstruction of macroscopic portions of the tissue at microscopic resolutions.

While there are several approaches to HRMac, for studies of collagen structural organization we have used vibratome sections from human corneas embedded in low melting point agarose and sectioned at 300-500 μm thick. These sections can extend from limbus-to-limbus and encompass the peripheral and central cornea. Sections are then mounted on glass coverslips and imaged using NLO SHG. Consecutive, high resolution image stacks are then acquired over the entire vibratome section using the Zeiss’ MultiTime macro function and large-scale mosaics concatenated into a single image stack using different software programs. Typical image data sets were comprised of 80 Mega Pixel image planes separated by 1-2 μm representing 16500 × 6500 pixels or 13.4 mm by 5.3 mm areas. File sizes were generally 64 Giga bytes in size.

Fig. 10A shows a zoomed-out HRMac image of the human cornea extending from the superior to inferior limbus. This magnification is similar to that of a standard low-powered stereo dissecting microscope image. Also shown are zoom-in images at full pixel resolution at the center of the cornea (B) and the limbal region where scleral collagen fibers enter the transparent cornea (C). This ability to zoom-in and zoom-out provides for “Google Maps” of the cornea where single collagen lamellae can be identified and followed for many millimeters within the corneal stroma. These structures can be easily extracted from the image stacks to generate three-dimensional representations of the corneal collagen organization to show how they interact with other collagen lamellae within the cornea. As shown in Fig. 11, anterior collagen lamellae that insert into the ALL appear to branch many times along their length. They also appear to combine with other collagen lamellae that also attach to the ALL creating what appears to be a three-dimensional ‘leaf spring’ that most likely has clear mechanical implications for the control of corneal shape. While past studies have shown that corneal collagen fibrils insert into the ALL (Mathew et al., 2008), in general these interactions are thought to be infrequent and limited to the ‘anterior corneal mosaic’ (Bron, 2001).

Extraction of lamellae from HRMac image data sets also identified two previously un-described collagen fiber structures, including long, prominent lamellae originating at or near the limbus that extend for millimeters across large portions of the cornea (Fig 12A, green fibers, arrow). These lamellae did not follow the corneal curvature from limbus-to-limbus; instead they seem to traverse many layers before terminating at or near the ALL. Interestingly, these fibers showed little branching or interaction with other lamellae when located deep in the corneal stroma, but show extensive interactions and branching as they traversed to the anterior cornea. A second type of collagen lamellae identified was the ‘bow spring’-like fibers that originate from the highly intertwined layers directly beneath the ALL and arc upwards, fusing with the layer itself before arcing back down (Fig. 12B and 12C, blue fibers, arrows). These lamellae were characterized by a near-parabolic shape, the apex of which is fused with the ALL.

Most importantly, three-dimensional reconstruction of lamellae in different depths of the cornea show distinctly different patterns, with anterior lamellae having complex branching and anastomosing patterns with many angled fibers running transverse to the corneal surface while posterior lamellae appear to run predominantly parallel to the surface with little branching (Fig. 13). This structural heterogeneity is consistent with the x-ray studies of (albeit swollen) human eye bank corneas alluded to earlier (Quantock et al., 2007). Interestingly, past studies of corneal swelling have shown that the anterior corneal stroma is resistant to swelling and maintains corneal shape as opposed to the posterior corneal stroma (Muller et al., 2001). It has been proposed that this unique property of the anterior cornea is related to the lamellar architecture, which would be more tightly interwoven in the anterior cornea as opposed to the posterior cornea (Bron, 2001; Muller et al., 2001). Our findings using HRMac to extract the three-dimensional organization supports and extends this hypothesis, in that lamellae in the anterior stroma are not only more tightly interwoven as in a basket weave pattern, but actually intertwined with extensive interactions with adjacent lamellae in three-dimensional space. This architectural design could lead to a much more rigid and mechanically stiff tissue that would aid in the maintenance of corneal shape. While swelling pressure is clearly different between anterior and posterior cornea, a major question is whether lamellar structure affects mechanical stiffness and rigidity of the cornea.

4.4 The Collagen Architecture and Mechanics of the Cornea

To relate corneal structure to tissue mechanics, the complexity of the collagen fiber patterns were first characterized in normal corneas. This has been performed in two separate studies, first using HRMac data sets from the center of the cornea in five normal eyes, and the second using HRMac data sets taken from the peripheral to central cornea in each of four quadrants (superior, inferior, nasal, temporal) of three eyes. Two different approaches have also been used to characterize collagen fiber complexity, the first assessing collagen fiber branching density and the second assessing collagen fiber angle relative to the corneal surface (Winkler et al., 2011; Winkler et al., 2013). In both studies, distinct and significant differences were detected between the complexity of the anterior compared to that of the middle and posterior cornea.

Regarding branching point density, the detected amount of lamellar branching was highest immediately below the ALL, reaching as high as 37 branches/mm or one every 20-30 μm. Density also showed a continuous though exponential decline, with the lowest number of branches detected just before the corneal endothelium averaging as low as 3 branches/mm. In the five corneas evaluated the anterior third of the cornea showed twice the branching density compared to the middle third ($p<0.01$) and almost four times the density compared to the posterior third ($p<0.01$).

In a second study, the lamellar angles were measured relative to the corneal surface. Since lamellar branching results in two divergent fibers, at least one fiber necessarily is angled relative to the corneal surface, and therefore characterizing fiber angles provides a measure of lamellar branching. Additionally, the angled fibers exert vectorial tensor effects within the tissue that can stiffen the response to compressive or shear strain. Using a computer automated approach to remove any subjective bias, lamellar angle was quantified as a function of radial location and depth. While the angle distribution remained significantly different in the anterior cornea, there were no differences detected in the radial distribution by region or quadrant. This finding confirmed the original data on depth distribution of lamellar branching, and suggested that there was little difference in the fiber architecture of the cornea from central to peripheral.

To assess the effects of collagen structure on mechanical tissue stiffness, tissue flaps of anterior, middle and posterior stroma were cut from fresh human donor corneas using a surgical femtosecond laser system. The tissue flaps were then mechanically tested using indentation and the effective elastic modulus calculated. Using this approach on seven donor corneas, the effective elastic modulus was significantly higher in the anterior stroma compared to the middle and posterior stroma by the same order of magnitude as that measured for branching point density or difference in fiber angle.

The finding that the anterior stroma is mechanically stiffer than the posterior cornea is consistent with more recent measurements using atomic force microscopy and shear modulus testing (Dias and Ziebarth, 2013; Last et al., 2012; Petsche and Pinsky, 2013) as well as the earlier empirical electron microscopy findings obtained from corneal swelling experiments (Muller et al., 2001). Together, these measurements strongly support the contention that the architectural organization of collagen plays an important role in defining tissue mechanics and hence corneal shape.

5. Summary Understandings and Future Directions

In this paper we have reviewed technologies that facilitate the evaluation and characterization of the ocular ECM spanning the Nano to the Macro scale; from WAXS to HRMac of SHG signals. With these methods we have gained novel insights into the hierarchical structure of the connective tissue of the eye, especially that of the cornea. Importantly, differences in collagen fibril diameter and spacing can be detected from the central to peripheral cornea using x-ray scattering, as can changes in the preferred collagen fibril orientation from superior-inferior/nasal-temporal central regions of the cornea to the more circumferential alignment peripherally. Using three-dimensional electron tomography

and SBF-SEM, new details of the cell and matrix structure are being discovered suggesting a cell-directed, complex organizational patterning of the stroma during development. Finally, NLO SHG and the development of MRMac have identified novel collagen lamellar patterns that suggest unique differences between anterior and posterior stroma that possibly contribute to differences in mechanical strength and the control of corneal shape. In the future, advancement of these technologies will lead to a more comprehensive hierarchical blueprint of the ocular ECMs that will provide essential insights of how the structural integrity of these connective tissues of the eye form, are maintained, and are affected and respond in disease or following surgery. In the short-to-medium term, this type of knowledge will provide insights into the structural changes underpinning corneal disorders, such as astigmatism and ectasia, and will also guide new research towards the drive to design and create a bioengineered corneal stroma.

Acknowledgments

Financial support: NIH grants EY07348, EY018665, EY016663, EY019719, The Discovery Eye Foundation, The Skirball Program in Molecular Ophthalmology, Support grant from Research to Prevent Blindness, Inc. Support for the Corneal Research Program at Cardiff University, led by Prof Keith Meek whom we acknowledge for helpful comments on this article, is provided by the UK government's Medical Research Council, Biotechnology and Biological Sciences Research Council and Engineering and Physical Sciences Research Council, as well as by charities, including Fight For Sight and The Wellcome Trust.

References

Abahussin M, Hayes S, Edelhauser H, Dawson D, Meek KM. A microscopy study of the structural features of post-LASIK human corneas. PLoS ONE. 2013; 8:e63268.10.1371/journal.pone.0063268 [PubMed: 23650559]

Abahussin M, Hayes S, Knox-Cartwright NE, Kamma-Lorger CS, Khan Y, Marshall J, Meek KM. 3D collagen orientation study of the human cornea using X-ray diffraction and femtosecond laser technology. Invest Ophthalmol Vis Sci. 2009; 50:5159–5164. [PubMed: 19516010]

Aghamohammadzadeh H, Newton RH, Meek KM. X-ray scattering used to map the preferred collagen orientation in the human cornea and limbus. Structure. 2004; 12:249–256. [PubMed: 14962385]

Akama TO, Nishida K, Nakayama J, Watanabe H, Ozaki K, Nakamura T, Dota A, Kawasaki S, Inoue Y, Maeda N, Yamamoto S, Fujiwara T, Thonar EJ, Shimomura Y, Kinoshita S, Tanigami A, Fukuda MN. Macular corneal dystrophy type I and type II are caused by distinct mutations in a new sulphotransferase gene. Nat Genet. 2000; 26:237–241. [PubMed: 11017086]

Akhtar S, Almubrad T, Paladini I, Menucci R. Keratoconus corneal architecture after riboflavin/ultraviolet A cross-linking: Ultrastructural studies. Mol Vis. 2013; 19:1526–1537. [PubMed: 23878503]

Allenspach AL. Ultrastructure of early chick embryo tissues after high pressure freezing and freeze substitution Microscopy res. technique. 1993; 24:369–384.

Aptel F, Olivier N, Deniset-Besseau A, Legeais JM, Plamann K, Schanne-Klein MC, Beaurepaire E. Multimodal nonlinear imaging of the human cornea. Invest Ophthalmol Vis Sci. 2010; 51:2459–2465. [PubMed: 20071677]

Austin BA, Coulon C, Liu CY, Kao WWY, Rada JA. Altered collagen fibril formation in the sclera of lumican-deficient mice. Invest Opthalmol Vis Sci. 2002; 43:1695–1701.

Baldock C, Koster AJ, Ziese U, Rock MJ, Sherratt MJ, Kadler KE, Shuttleworth CA, Kielty CM. The supramolecular organization of fibrillin-rich microfibrils. J Cell Biol. 2001; 152:10451056.

Beecher N, Carlson C, Allen BR, Kipchumba R, Conrad GW, Meek KM, Quantock AJ. An x-ray diffraction study of corneal structure in mimecan-deficient mice. Invest Ophthalmol Vis Sci. 2005; 46:4046–4050. [PubMed: 16249479]

Beecher N, Chakravarti S, Joyce S, Meek KM, Quantock AJ. Neonatal development of the corneal stroma in wild-type and lumican-null mice. Invest Ophthalmol Vis Sci. 2006; 47:146–150. [PubMed: 16384956]

Birk DE, Fitch JM, Babiarz JP, Linsenmeyer TF. Collagen type I and type V are present in the same fibril in the avian corneal stroma. J Cell Biol. 1988; 106:999–1008. [PubMed: 3346334]

Birk DE, Trelstad RL. Extracellular compartments in matrix morphogenesis: Collagen fibril, bundle, and lamellar formation by corneal fibroblasts. J Cell Biol. 1984; 99:2024–2033. [PubMed: 6542105]

Blochberger TC, Vergnes JP, Hempel J, Hassell JR. cDNA to chick lumican (corneal keratan sulfate proteoglycan) reveals homology to the small interstitial proteoglycan gene family and expression in muscle and intestine. J Biol Chem. 1992; 267:347–352. [PubMed: 1370446]

Boote C, Du Y, Morgan SR, Harris J, Kamma-Lorger CS, Hayes S, Lathrop KL, Roh DS, Burrow MK, Hiller J, Terrill NJ, Funderburgh JL, Meek KM. Quantitative Assessment of Ultrastructure and Light Scatter in Mouse Corneal Debridement Wounds. Invest Ophthalmol Vis Sci. 2012; 53:2786–2795. [PubMed: 22467580]

Boote C, Hayes S, Abahussin M, Meek KM. Mapping collagen organisation in the human cornea: left and right eyes are structurally distinct. Invest Ophthalmol Vis Sci. 2006; 47:901–908. [PubMed: 16505022]

Boote C, Hayes S, Jones S, Quantock AJ, Hocking PM, Inglehearn CF, Ali M, Meek KM. Collagen organization in the chicken cornea and structural alterations in the retinopathy, globe enlarged (rge) phenotype--an X-ray diffraction study. J Struct Biol. 2008; 161:1–8. [PubMed: 17936639]

Boote C, Hayes S, Young RD, Kamma-Lorger CS, Hocking PM, Elsheikh A, Inglehearn CF, Ali M, Meek KM. Ultrastructural changes in the retinopathy, globe enlarged (rge) chick cornea. J Struct Biol. 2009; 166:195–204. [PubMed: 19258040]

Boote C, Kamma-Lorger CS, Hayes S, Harris J, Burghammer M, Hiller J, Terrill NJ, Meek KM. Quantification of collagen organization in the peripheral human cornea at micron-scale resolution. Biophys J. 2011; 101:33–42. [PubMed: 21723812]

Boote C, Siegler V, Meek KM, Quantock AJ. A wide-angle x-ray diffraction study of the developing embryonic chicken cornea. Fibre Diffraction Rev. 2003; 11:123–129.

Borcherding MS, Blacik LJ, Sittig RA, Bizzell JW, Breen M, Weinstein HG. Proteoglycans and collagen fibre organization in human corneoscleral tissue. Exp Eye Res. 1975; 21:59–70. [PubMed: 124659]

Bowman, W. Lectures on the parts concerned in the operations on the eye, and on the structure of the retina. Longman, Brown, Green, and Longmans; London: 1849.

Bron AJ. The architecture of the corneal stroma. The British journal of ophthalmology. 2001; 85:379–381. [PubMed: 11264120]

Bron, AJ.; Tripathi, RC.; Tripathi, BJ. Wolff's Anatomy of the Eye and Orbit. Eighth. Chapman & Hall Medical; London, Weinheim, New York, Tokyo, Melbourne, Madras: 1997.

Bueno EM, Saeidi N, Melotti S, Ruberti JW. Effect of serum and insulin modulation on the organization and morphology of matrix synthesized by bovine corneal stromal cells. Tissue Eng Part A. 2009; 15:3559–3573. [PubMed: 19480568]

Bueno JM, Gualda EJ, Giakoumaki A, Perez-Merino P, Marcos S, Artal P. Multiphoton microscopy of ex vivo corneas after collagen cross-linking. Invest Ophthalmol Vis Sci. 2011; 52:5325–5331. [PubMed: 21467175]

Bushby AJ, Png KMY, Young RD, Pinali C, Knupp C, Quantock AJ. Imaging three-dimensional tissue architectures by focused ion beam scanning electron microscopy. Nat Protoc. 2011; 6:845–858. [PubMed: 21637203]

Caterson B, Christner JE, Baker JR. Identification of a monoclonal antibody that specifically recognises corneal and skeletal keratin sulphate. J Biol Chem. 1983; 258:8848–8854. [PubMed: 6223038]

Caterson B, Christner JE, Baker JR, Couchman JR. Production and characterization of monoclonal antibodies directed against connective tissue proteoglycans. Fed Proc. 1985; 44:386–393. [PubMed: 2578417]

Chakravarti S, Magnuson T, Lass JH, Jepsen KJ, LaMantia C, Carroll H. Lumican regulates collagen fibril assembly: skin fragility and corneal opacity in the absence of lumican. J Cell Biol. 1998; 5:1277–1286. [PubMed: 9606218]

Chakravarti S, Petroll WM, Hassell JR, Jester JV, Lass JH, Paul J, Birk DE. Corneal opacity in lumican-null mice: defects in collagen fibril structure and packing in the posterior stroma. Invest Ophthalmol Vis Sci. 2000; 41:3365–3373. [PubMed: 11006226]

Chen S, Oldberg A, Chakravarti S, Birk DE. Fibromodulin regulates collagen fibrillogenesis during peripheralcorneal development. Dev Dyn. 2010; 239:844–854. [PubMed: 20108350]

Cintron C, Covington HI. Proteoglycan distribution in developing rabbit cornea. J Histochem Cytochem. 1990; 38:675–684. [PubMed: 2332625]

Cintron C, Szaimier RB, Hassinger LC, Kublin CL. Scanning Electron microscopy of rabbit corneal scars. Invest Opthalmol Vis Sci. 1982; 23:50–63.

Connon CJ, Marshall J, Patmore AL, Brahma A, Meek KM. Persistent haze and disorganization of anterior stromal collagen appear unrelated following phototherapeutic keratectomy. J Refract Surg. 2003a; 19:323–332. [PubMed: 12777028]

Connon CJ, Meek KM, Newton RH, Kenney MC, Alba SA, Karageozian H. Hyaluronidase treatment of the cornea results in compression of collagen fibril packing but normal transparency. J Refract Surg. 2000; 16:448–55. [PubMed: 10939725]

Connon CJ, Siegler V, Meek KM, Hodson SA, Caterson B, Kinoshita S, Quantock AJ. Proteoglycan alterations and collagen reorganisation in the secondary avian cornea during development. Ophthalmic Res. 2003b; 55:177–184. [PubMed: 12815192]

Corpuz LM, Funderburgh JL, Funderburgh ML, Bottomley GS, Prakash S, Conrad GW. Molecular cloning and tissue distribution of keratocan. Bovine corneal keratan sulfate proteoglycan 37A. J Biol Chem. 1996; 271:9759–9763. [PubMed: 8621655]

Coudrillier B, Boote C, Quigley HA, Nguyen TD. Scleral anisotropy and its effects on the mechanical response of the optic nerve head. Biomech Model Mechanobiol. 2013; 12:941–963. [PubMed: 23188256]

Coulombre AJ, Coulombre JL. Corneal development I. Corneal transparency. J Cell Comp Physiol. 1958; 51:1–11.

Craig AS, Robertson JG, Parry DA. Preservation of corneal fibril structure using low-temperature procedures for electron microscopy. J Ultrastruct Mol Struct Res. 1986; 96:172–175. [PubMed: 3119734]

Danielson KG, Baribault H, Holmes DF, Graham H, Kadler KE, Iozzo RV. Targeted disruption of decorin leads to abnormal collagen fibril morphology and skin fragility. The Journal of cell biology. 1997; 136:729–743. [PubMed: 9024701]

Davies Y, Fullwood NJ, Marcyniuk B, Bonshek R, Tullo A, Nieduszynski IA. Keratan sulphate in the trabecular meshwork and cornea. Curr Eye Res. 1997; 16:677–686. [PubMed: 9222085]

Daxer A, Fratzl P. Collagen fibril orientation in the human corneal stroma and its implications in keratoconus. Invest Ophthalmol Vis Sci. 1997; 38:121–129. [PubMed: 9008637]

Daxer A, Misof K, Grabner B, Ettl A, Fratzl P. Collagen fibrils in the human corneal stroma: structure and ageing. Invest Ophthalmol Vis Sci. 1998; 39:644–648. [PubMed: 9501878]

Denk W, Horstmann H. Serial block-face scanning electron microscopy to reconstruct three-dimensional tissue nanostructure. PLoS Biol. 2004; 2:e329. [PubMed: 15514700]

Dias JM, Ziebarth NM. Anterior and posterior corneal stroma elasticity assessed using nanoindentation. Experimental eye research. 2013; 115:41–46. [PubMed: 23800511]

Donnenfeld ED, Cohen EJ, Ingraham HJ, Poleski SA, Goldsmith E, Laibson PR. Corneal thinning in macular corneal dystrophy. Am J Ophthalmol. 1986; 101:112–113. [PubMed: 3484610]

Ehlers N, Bramsen T. Central thickness in corneal disorders. Acta Ophthalmol. 1978; 56:412–416. [PubMed: 308291]

Elliott GF, Hodson SA. Cornea, and the swelling of polyelectrolyte gels of biological interest. Rep Prog Phys. 1998; 61:1325–1365.

Elliott GF, Goodfellow JM, Woolgar AE. Swelling studies of bovine corneal stroma without bounding membranes. J Physiol. 1980; 298:453–470. [PubMed: 7359427]

Elliott GF, Sayers Z, Timmins PA. Neutron diffraction studies of the corneal stroma. J Mol Biol. 1982; 155:389–393. [PubMed: 7077678]

Farid M, Morishige N, Lam L, Wahlert A, Steinert RF, Jester JV. Detection of corneal fibrosis by imaging second harmonic-generated signals in rabbit corneas treated with mitomycin C after excimer laser surface ablation. Invest Ophthalmol Vis Sci. 2008; 49:4377–4383. [PubMed: 18502995]

Faulk WP, Taylor GM. An immunocolloid method for the electron microscope. Immunochem. 1971; 8:1081–1083.

Federative Committee on Anatomical Terminology (FCAT). Terminologia Anatomica. Stuttgart: Thieme; 1998.

Franken P, Hill A, Peters C, Weinreich G. Generation of optical harmonics. Phys Rev Lett. 1961; 7:118–119.

Fratzl P, Daxer A. Structural transformation of collagen fibrils in corneal stroma during drying. An x-ray scattering study. Biophys J. 1993; 64:1210–1214. [PubMed: 8494978]

Fullwood NJ, Meek KM. A synchrotron X-ray study of the changes occurring in the corneal stroma during processing for electron microscopy. J Microsc. 1993; 169:53–60. [PubMed: 8445631]

Fullwood NJ, Tuft SJ, Malik NS, Meek KM, Ridgway AEA, Harrison RJ. Synchrotron x-ray diffraction studies of keratoconus corneal stroma. Invest Ophthalmol Vis Sci. 1992; 33:1734–1741. [PubMed: 1559773]

Funderburgh JL, Corpuz LM, Roth MR, Funderburgh ML, Tasheva ES, Conrad GW. Mimecan, the 25-kDa corneal keratan sulfate proteoglycan, is a product of the gene producing osteoglycin. J Biol Chem. 1997; 272:28089–28095. [PubMed: 9346963]

Ghazaryan A, Tsai HF, Hayrapetyan G, Chen WL, Chen YF, Jeong MY, Kim CS, Chen SJ, Dong CY. Analysis of collagen fiber domain organization by Fourier second harmonic generation microscopy. Journal of Biomedical Optics. 2013; 18:31105. [PubMed: 23174951]

Glauert AM, Glauert RH, Rogers GE. A new embedding medium for electron microscopy. Nature. 1956; 178:803. [PubMed: 13369546]

Goodfellow JM, Elliott GF, Woolgar AE. X-ray diffraction studies of the corneal stroma. J Mol Biol. 1978; 119:237–252. [PubMed: 24753]

Goppert-Mayer M. Uber Elementarakte mit zweit quantensprungen. Ann Phys. 1931; 9:273–294.

Gyi TJ, Meek KM, Elliott GF. Collagen interfibrillar distances in corneal stroma using synchrotron X-ray diffraction: A species study. Int J Biol Macromol. 1988; 10:265–269.

Hamada R, Giraud JP, Graf B, Pouliquen Y. Analytical and statistical study of the lamellae, keratocytes and collagen fibrils of the central region of the normal human cornea. (Light and electron microscopy). Archives d'ophtalmologie et revue generale d'ophtalmologie. 1972; 32:563–570.

Han M, Giese G, Bille J. Second harmonic generation imaging of collagen fibrils in cornea and sclera. Optics express. 2005; 13:5791–5797. [PubMed: 19498583]

Han M, Zickler L, Giese G, Walter M, Loesel FH, Bille JF. Second-harmonic imaging of cornea after intrastromal femtosecond laser ablation. Journal of biomedical optics. 2004; 9:760–766. [PubMed: 15250763]

Hassell JR, Cintron C, Kublin C, Newsome DA. Proteoglycan changes during restoration of transparency in corneal scars. Arch Biochem Biophys. 1983; 222:362–369. [PubMed: 6847191]

Hay, E.; Revel, JP. Fine structure of the developing avian cornea. Monographs in Developmental Biology. S Karger; New York: 1969.

Hay ED. Development of the vertebrate cornea. Int Rev Cytol. 1979; 63:263–322. [PubMed: 395131]

Hayashida Y, Akama TO, Beecher N, Lewis P, Young RD, Meek KM, Kerr B, Hughes CE, Caterson B, Tanigami A, Nakayama J, Fukada MN, Tano Y, Nishida K, Quantock AJ. Matrix morphogenesis in cornea is mediated by the modification of keratan sulfate by GlcNAc 6-O sulfotransferase. Proc Natl Acad Sci U S A. 2006; 103:13333–13338. [PubMed: 16938851]

Hayes S, Boote C, Lewis J, Sheppard J, Abahussin M, Quantock AJ, Purslow C, Votruba M, Meek KM. Comparative study of fibrillar collagen arrangement in the corneas of primates and other animals. Anat Rec (Hoboken). 2007b; 290:1542–1550. [PubMed: 17957749]

Hayes S, Boote C, Tuft SJ, Quantock AJ, Meek KM. A study of corneal thickness, shape and collagen organisation in keratoconus using videokeratography and X-ray scattering techniques. Exp Eye Res. 2007a; 84:423–434. [PubMed: 17178118]

Hayes S, Kamma-Lorger CS, Boote C, Young RD, Quantock AJ, Rost A, Khatib Y, Harris J, Yagi N, Terrill N, Meek KM. The effect of riboflavin/UVA collagen cross-linking therapy on the structure and hydrodynamic behaviour of the ungulate and rabbit corneal stroma. PLoS One. 2013; 8:e52860. [PubMed: 23349690]

Hayes S, Khan S, Boote C, Kamma-Lorger CS, Dooley E, Lewis J, Hawksworth N, Sorensen T, Daya S, Meek KM. Depth profile study of abnormal collagen orientation in keratoconus corneas. Arch Ophthalmol. 2012; 130:251–252. [PubMed: 22332225]

Hirsch M, Prenant G, Renard G. Three-dimensional supramolecular organization of the extracellular matrix in human and rabbit corneal stroma, as revealed by ultrarapid freezing and deep-etch methods. Exp Eye Res. 2001; 72:123–135. [PubMed: 11161728]

Hochheimer BF. Second harmonic light generation in the rabbit cornea. Applied optics. 1982; 21:1516–1518. [PubMed: 20389884]

Hodson SA. Corneal stromal swelling. Prog Ret Eye Res. 1997; 16:99–116.

Hogan, MJ.; Alvarado, JA.; Weddell, J. Histology of the human eye. WB Saunders; Philadelphia: 1971.

Holmes DF, Gilpin CJ, Baldock C, Ziese U, Koster AJ, Kadler KE. Corneal collagen fibril structure in three dimensions: structural insights into fibril assembly, mechanical properties, and tissue organization. Proc Nat Acad Sci. 2001; 111:687–692.

Hsueh CM, Lo W, Chen WL, Hovhannisyan VA, Liu GY, Wang SS, Tan HY, Dong CY. Structural characterization of edematous corneas by forward and backward second harmonic generation imaging. Biophysical journal. 2009; 97:1198–1205. [PubMed: 19686668]

Huang Y, Bron AJ, Meek KM, Vellodi A, McDonald B. Ultrastructural study of the cornea in a bone marrow-transplanted Hurler syndrome patient. Exp Eye Res. 1996; 62:377–387. [PubMed: 8795456]

Huang Y, Meek KM. Swelling studies on the cornea and sclera: the effects of pH and ionic strength. Biophys J. 1999; 77:1655–1665. [PubMed: 10465776]

Hughes L, Hawes C, Monteith S, Vaughan S. Serial block face scanning electron microscopy-the future of cell ultrastructure imaging. Protoplasma. 2014; 251:395–401. [PubMed: 24240569]

Hulmes DJS, Miller A. Quasi-hexagonal molecular packing in collagen fibrils. Nature. 1979; 282:878–880. [PubMed: 514368]

Jakus MA. Studies on the cornea. 1. The fine structure of the rat cornea. Am J Ophthalmol. 1954; 38:40–53. [PubMed: 13180617]

Jay L, Brocas A, Singh K, Kieffer JC, Brunette I, Ozaki T. Determination of porcine corneal layers with high spatial resolution by simultaneous second and third harmonic generation microscopy. Optics express. 2008; 16:16284–16293. [PubMed: 18852734]

Kamma-Lorger CS, Boote C, Hayes S, Albon J, Boulton ME, Meek KM. Collagen ultrastructural changes during stromal wound healing in organ cultured bovine corneas. Experimental Eye Research. 2009b; 88:953–959. [PubMed: 19133259]

Kamma-Lorger CS, Boote C, Hayes S, Moger J, Burghammer M, Knupp C, Quantock AJ, Sorensen T, Cola ED, White N, Young RD, Meek KM. Collagen and mature elastic fibre organisation as a function of depth in the human cornea and limbus. J Struct Biol. 2010; 169:424–430. [PubMed: 19914381]

Kamma-Lorger CS, Hayes S, Boote C, Burghammer M, Boulton ME, Meek KM. Effects on collagen orientation in the cornea after trephine injury. Molecular Vision. 2009a; 15:378–385. [PubMed: 19234631]

Knott G, Marchman H, Wall D, Lich B. Serial section scanning electron microscopy of adult brain tissue using focused ion beam milling. J Neurosci. 2008; 28:2959–2964. [PubMed: 18353998]

Knupp C, Chong NH, Munro PM, Luthert PJ, Squire JM. Analysis of the collagen VI assemblies associated with Sorsby's fundus dystrophy. J Struct Biol. 2002; 137:31–40. [PubMed: 12064931]

Knupp C, Munro PM, Luther PK, Ezra E, Squire JM. Structure of abnormal molecular assemblies (collagen VI) associated with human full thickness macular holes. J Struct Biol. 2000; 129:38–47. [PubMed: 10675295]

Knupp C, Pinali C, Munro PM, Gruber HE, Sherratt MJ, Baldock C, Squire JM. Structural correlation between collagen VI microfibrils and collagen VI banded aggregates. J Struct Biol. 2006; 154:312–326. [PubMed: 16713302]

Kokott W. Uber mechanisch-funktionelle strukturen des auges. Albrecht van Graefes Archiv fur Ophthalmologie. 1938; 138:424–485.

Komai Y, Ushiki T. The three-dimensional organization of collagen fibrils in the human cornea and sclera. Invest Ophthalmol Vis Sci. 1991; 32:2244–2258. [PubMed: 2071337]

Last JA, Thomasy SM, Croasdale CR, Russell P, Murphy CJ. Compliance profile of the human cornea as measured by atomic force microscopy. Micron. 2012; 43:1293–1298. [PubMed: 22421334]

Latour G, Gusachenko I, Kowalczuk L, Lamarre I, Schanne-Klein MC. In vivo structural imaging of the cornea by polarization-resolved second harmonic microscopy. Biomedical optics express. 2012a; 3:1–15. [PubMed: 22254163]

Latour G, Kowalczuk L, Savoldelli M, Bourges JL, Plamann K, Behar-Cohen F, Schanne-Klein MC. Hyperglycemia-induced abnormalities in rat and human corneas: the potential of second harmonic generation microscopy. PloS one. 2012b; 7:e48388. [PubMed: 23139780]

Lau TY, Ambekar R, Toussaint KC. Quantification of collagen fiber organization using three-dimensional Fourier transform-second-harmonic generation imaging. Optics express. 2012; 20:21821–21832. [PubMed: 23037302]

Leonard DW, Meek KM. Refractive indices of the collagen fibrils and extrafibrillar material of the corneal stroma. Biophys J. 1997; 72:1382–1387. [PubMed: 9138583]

Lewis D, Davies Y, Nieduszynski IA, Lawrence F, Quantock AJ, Bonshek R, Fullwood NJ. Ultrastructural localization of sulfated and unsulfated keratan sulfate in normal and macular corneal dystrophy type I. Glycobiology. 2000; 10:305–312. [PubMed: 10704529]

Lewis PN, Pinali C, Young RD, Meek KM, Quantock AJ, Knupp C. Structural interactions between collagen and proteoglycans are elucidated by three-dimensional electron tomography of bovine cornea. Structure. 2010; 18:1–7. [PubMed: 20152144]

Li W, Vergnes JP, Cornuet PK, Hassell JR. cDNA clone to chick corneal chondroitin dermatan sulfate proteoglycan reveals identity to decorin. Arch Biochem Biophys. 1992; 296:190–197. [PubMed: 1605630]

Liles M, Palka B, Harris A, Kerr B, Hughes C, Young RD, Meek KM, Caterson B, Quantock AJ. Differential relative sulfation of keratan sulphate glycosaminoglycan in the chick cornea during embryonic development. Invest Ophthalmol Vis Sci. 2010; 51:1365–1372. [PubMed: 19815728]

Linsenmayer TF, Fitch JM, Gordon MK, Cai CX, Igoe F, Marchant JK, Birk DE. Development and roles of collagenous matrices in the embryonic avian cornea. Prog Retin Eye Res. 1998; 17:231–265. [PubMed: 9695794]

Liu CY, Birk DE, Hassell JR, Kane B, Kao WWY. Keratocan-deficient mice display alterations in corneal structure. J Biol Chem. 2003; 278:21672–21677. [PubMed: 12665512]

Lo W, Chang YL, Liu JS, Hseuh CM, Hovhannisyan V, Chen SJ, Tan HY, Dong CY. Multimodal, multiphoton microscopy and image correlation analysis for characterizing corneal thermal damage. Journal of biomedical optics. 2009; 14:054003. [PubMed: 19895105]

Lo W, Chen WL, Hsueh CM, Ghazaryan AA, Chen SJ, Ma DH, Dong CY, Tan HY. Fast Fourier transform-based analysis of second-harmonic generation image in keratoconic cornea. Invest Ophthalmol Vis Sci. 2012; 53:3501–3507. [PubMed: 22570347]

Lo W, Teng SW, Tan HY, Kim KH, Chen HC, Lee HS, Chen YF, So PT, Dong CY. Intact corneal stroma visualization of GFP mouse revealed by multiphoton imaging. Microscopy research and technique. 2006; 69:973–975. [PubMed: 16972234]

Lütjen-Drecoll E. Functional morphology of the trabecular meshwork in primate eyes. Prog Retin Eye Res. 1999; 18:91–119. [PubMed: 9920500]

Lyubovitsky JG, Spencer JA, Krasieva TB, Andersen B, Tromberg BJ. Imaging corneal pathology in a transgenic mouse model using nonlinear microscopy. Journal of biomedical optics. 2006; 11:014013. [PubMed: 16526890]

Malik NS, Meek KM. The inhibition of sugar-induced structural alterations in collagen by asprin and other compounds. Biochem Biophys Res Commun. 1994; 199:683–686. [PubMed: 8135810]

Malik NS, Meek KM. Vitamins and analgesics in the prevention of collagen ageing. Age Ageing. 1996; 25:279–284. [PubMed: 8831872]

Malik NS, Moss SJ, Ahmed N, Furth AJ, Wall RS, Meek KM. Ageing of the human corneal stroma: structural and biochemical changes. Biochim Biophys Acta. 1992; 1138:222–228. [PubMed: 1547284]

Marchini M, Morocutti M, Ruggeri A, Koch MHJ, Bigi A, Roveri N. Differences in the fibril structure of corneal and tendon collagen. An electron microscopy and x-ray diffraction investigation. Connective Tissue Res. 1986; 15:269–281.

Marshall GE, Konstas AG, Lee WR. Immunogold fine structural localization of extracellular matrix components in aged human cornea.1. Types I-IV collagen and laminin. Graefe's Arch Clin Exp Ophthalmol. 1991; 229:157–163. [PubMed: 2044978]

Marshall GE, Konstas AG, Lee WR. Collagens in ocular tissues. Brit J Ophthalmol. 1993; 77:515–524. [PubMed: 8025051]

Martell JD, Deerinck TJ, Sancak Y, Poulos TL, Mootha VK, Sosinsky GE, Ellisman MH, Ting AY. Engineered ascorbate peroxidase as a genetically encoded reporter for electron microscopy. Nat Biotechnol. 2012; 30:1143–1148. [PubMed: 23086203]

Mathew JH, Bergmanson JP, Doughty MJ. Fine structure of the interface between the anterior limiting lamina and the anterior stromal fibrils of the human cornea. Invest Ophthalmol Vis Sci. 2008; 49:3914–3918. [PubMed: 18765633]

Maurice DM. The structure and transparency of the cornea. J Physiol. 1957; 136:263–286. [PubMed: 13429485]

Maurice DM. Clinical physiology of the cornea. Int Ophthalmol Clin. 1962; 2:561–572. [PubMed: 13934004]

Meek KM, Blamires T, Elliott GF, Gyi T, Nave C. The organisation of collagen fibrils in the human corneal stroma: A synchrotron X-ray diffraction study. Curr Eye Res. 1987; 6:841–846. [PubMed: 3621979]

Meek KM, Boote C. The use of x-ray scattering techniques to quantify the orientation and distribution of collagen in the corneal stroma. Prog Retin Eye Res. 2009; 28:369–392. [PubMed: 19577657]

Meek KM, Elliott GF, Nave C. A synchrotron X-ray diffraction study of bovine cornea stained with Cupromeronic blue. Coll Relat Res. 1986; 6:203–218. [PubMed: 3731748]

Meek KM, Elliott GF, Sayers Z, Whitburn SB, Koch MHJ. Interpretation of the meridional X-ray diffraction pattern from collagen fibrils in corneal stroma. J Mol Biol. 1981; 149:477–488. [PubMed: 7310887]

Meek KM, Fullwood NJ, Cooke PH, Elliott GF, Maurice DM, Quantock AJ, Wall RS, Worthington CR. Synchrotron x-ray diffraction studies of the cornea with implications for stromal hydration. Biophys J. 1991; 60:467–474. [PubMed: 1912282]

Meek KM, Leonard DW. The ultrastructure of the corneal stroma: a comparative study. Biophys J. 1993; 64:273–280. [PubMed: 8431547]

Meek KM, Newton RH. Organisation of collagen fibrils in the corneal stroma in relation to mechanical properties and surgical practice. J Refract Surg. 1999; 15:695–699. [PubMed: 10590012]

Meek KM, Quantock AJ. The use of x-ray scattering techniques to determine corneal ultrastructure. Prog, Ret, Eye Res. 2001; 20:95–137.

Meek KM, Quantock AJ, Boote C, Liu CY, Kao WWY. An x-ray scattering investigation of corneal structure in keratocan-deficient mice. Matrix Biol. 2003; 22:467–475. [PubMed: 14667839]

Meek KM, Tuft SJ, Huang Y, Gill PS, Hayes S, Newton RH, Bron AJ. Changes in collagen orientation and distribution in keratoconus corneas. Invest Ophthalmol Vis Sci. 2005; 46:1948–1956. [PubMed: 15914608]

Mega Y, Robitaille M, Zareian R, McLean J, Ruberti J, DiMarzio C. Quantification of lamellar orientation in corneal collagen using second harmonic generation images. Optics letters. 2012; 37:3312–3314. [PubMed: 23381241]

Morgan SR, Dooley EP, Hocking PM, Inglehearn CF, Ali M, Sorensen TL, Meek KM, Boote C. An x-ray scattering study into the structural basis of corneal refractive function in an avian model. Biophys J. 2013; 104:2586–2594. [PubMed: 23790366]

Morishige N, Petroll WM, Nishida T, Kenney MC, Jester JV. Noninvasive corneal stromal collagen imaging using two-photon-generated second-harmonic signals. J Cataract Refract Surg. 2006; 32:1784–1791. [PubMed: 17081858]

Morishige N, Wahlert AJ, Kenney MC, Brown DJ, Kawamoto K, Chikama T, Nishida T, Jester JV. Second-harmonic imaging microscopy of normal human and keratoconus cornea. Invest Ophthalmol Vis Sci. 2007; 48:1087–1094. [PubMed: 17325150]

Muller LJ, Pels E, Schurmans LR, Vrensen GF. A new three dimensional model of the organization of proteoglycans and collagen fibrils in corneal stroma. Exp Eye Res. 2004; 78:493–501. [PubMed: 15106928]

Muller LJ, Pels E, Vrensen GF. The specific architecture of the anterior stroma accounts for maintenance of corneal curvature. The British journal of ophthalmology. 2001; 85:437–443. [PubMed: 11264134]

Newton RH, Meek KM. Circumcorneal annulus of collagen fibrils in the human limbus. Invest Ophthalmol Vis Sci. 1998a; 39:1125–1134. [PubMed: 9620071]

Newton RH, Meek KM. The integration of the corneal and limbal fibrils in the human eye. Biophys J. 1998b; 75:2508–2512. [PubMed: 9788946]

Nien CJ, Flynn KJ, Chang M, Brown D, Jester JV. Reducing peak corneal haze after photorefractive keratectomy in rabbits: prednisolone acetate 1.00% versus cyclosporine A 0.05%. J Cataract Refract Surg. 2011; 37:937–944. [PubMed: 21406325]

Nishida T, Yasumoto K, Orori T, Desaki J. The network structure of corneal fibroblasts in the rat as revealed by scanning electron microscopy. Invest Ophthalmol Vis Sci. 1988; 29:1887–1890. [PubMed: 3192380]

Orgel JP, Wess TJ, Miller A. The in situ conformation and axial location of the intermolecular cross-linked non-helical telopeptides of type I collagen. Structure. 2000; 8:137–142. [PubMed: 10673433]

Palka BP, Sotozono C, Tanioka H, Akama TO, Yagi N, Boote C, Young RD, Meek KM, Kinoshita S, Quantock AJ. Structural collagen alterations in macular corneal dystrophy occur mainly in the posterior stroma. Curr, Eye Res. 2010; 35:580–586. [PubMed: 20597644]

Parfitt GJ, Pinali C, Akama TO, Young RD, Nishida K, Quantock AJ, Knupp C. Electron tomography reveals multiple self-association of chondroitin/dermatan sulphate proteoglycans in Chst5-null mouse corneas. J Struct Biol. 2011; 174:536–541. [PubMed: 21440637]

Parfitt GJ, Pinali C, Young RD, Quantock AJ, Knupp C. Three-dimensional reconstruction of collagen-proteoglycan interactions in the mouse corneal stroma by electron tomography. J Struct Biol. 2010; 170:392–397. [PubMed: 20132890]

Petsche SJ, Pinsky PM. The role of 3-D collagen organization in stromal elasticity: a model based on X-ray diffraction data and second harmonic-generated images. Biomechanics and modeling in mechanobiology. 2013; 12:1101–1113. [PubMed: 23288406]

Pijanka JK, Abass A, Sorensen T, Elsheikh A, Boote C. A wide-angle X-ray fibre diffraction method for quantifying collagen orientation across large tissue areas: application to the human eyeball coat. J Appl Crystallogr. 2013; 46:1481–1489.

Pijanka JK, Coudrillier B, Ziegler K, Sorensen T, Meek KM, Nguyen TD, Quigley HA, Boote C. Quantitative mapping of collagen fiber orientation in non-glaucoma and glaucoma posterior human sclerae. Invest Ophthalmol Vis Sci. 2012; 53:5258–5270. [PubMed: 22786908]

Pinsky PM, Van der Heide D, Chernyak D. Computational modeling of mechanical anisotropy in the cornea and sclera. J Cataract Refract Surg. 2005; 31:136–145. [PubMed: 15721706]

Polack FM. Contributions of electron microscopy to the study of corneal pathology. Survey of ophthalmology. 1976; 20:375–414. [PubMed: 779087]

Powner MB, Scott A, Zhu M, Munro PM, Foss AJ, Hageman GS, Gillies MC, Fruttiger M. Basement membrane changes in capillaries of the ageing human retina. Br J Ophthalmol. 2011; 95:1316–22. [PubMed: 21606466]

Prakash S, Conrad GW. Molecular cloning and tissue distribution of keratocan. Bovine corneal keratan sulfate proteoglycan 37A. J Biol Chem. 1996; 271:9759–9763. [PubMed: 8621655]

Quantock AJ, Boote C, Siegler V, Meek KM. Collagen organization in the secondary chick cornea during development. Invest Ophthalmol Vis Sci. 2003a; 44:130–136. [PubMed: 12506065]

Quantock AJ, Boote C, Young RD, Hayes S, Tanioka H, Kawasaki S, Ohta N, Iida T, Yagi N, Kinoshita S, Meek KM. Small-angle fibre diffraction studies of corneal matrix structure: a depth-profiled investigation of the human eye-bank cornea. J Appl Crystal. 2007; 40:335–340.

Quantock AJ, Dennis S, Adachi W, Kinoshita S, Boote C, Meek KM, Matsushima Y, Tachibana M. Annulus of collagen fibrils in mouse cornea and structural matrix alterations in a murine-specific keratopathy. Invest Ophthalmol Vis Sci. 2003b; 44:1906–1911. [PubMed: 12714622]

Quantock AJ, Fullwood NJ, Thonar EJMA, Waltman SR, Capel MC, Ito M, Verity SM, Schanzlin DJ. Macular corneal dystrophy type II: Multiple studies on a cornea with low levels of sulphated keratan sulphate. Eye. 1997a; 11:57–67. [PubMed: 9246278]

Quantock AJ, Kinoshita S, Capel MS, Schanzlin DJ. A synchrotron x-ray diffraction study of developing chick corneas. Biophys J. 1998; 74:995–998. [PubMed: 9533711]

Quantock AJ, Klintworth GK, Schanzlin DJ, Capel MC, Lenz ME, Thonar EJMA. Proteoglycans contain a 4.6A repeat in macular dystrophy corneas: X-ray diffraction evidence. Biophys J. 1996; 70:1966–1972. [PubMed: 8785355]

Quantock AJ, Klintworth GK, Schanzlin DJ, Lenz ME, Thonar EJMA. Proteoglycans contain a 4.6A repeat in corneas with macular dystrophy: II. Histochemical evidence. Cornea. 1997b; 16:322–327. [PubMed: 9143806]

Quantock AJ, Meek K, Thonar EJ. Analysis of high-angle synchrotron x-ray diffraction patterns obtained from macular dystrophy corneas. Cornea. 1992; 11:185–190. [PubMed: 1587124]

Quantock AJ, Meek KM. Axial electron density of human scleral collagen: Location of proteoglycans by x-ray diffraction. Biophys J. 1988; 54:159–164. [PubMed: 3416025]

Quantock AJ, Meek KM, Chakravarti S. An x-ray diffraction investigation of corneal structure in lumican-deficient mice. Invest Ophthalmol Vis Sci. 2001; 42:1750–1756. [PubMed: 11431438]

Quantock AJ, Meek KM, Fullwood NJ, Zabel RW. Scheie's syndrome: The architecture of corneal collagen and distribution of corneal proteoglycans. Can J Ophthalmol. 1993b; 28:266–272. [PubMed: 8299051]

Quantock AJ, Meek KM, Ridgway AEA, Bron AJ, Thonar EJMA. Macular corneal dystrophy: Reduction in both corneal thickness and collagen interfibrillar spacing. Curr Eye Res. 1990; 9:393–398. [PubMed: 2340750]

Quantock AJ, Meek KM, Thonar EJMA, Assil KK. Synchrotron x-ray diffraction in atypical macular dystrophy. Eye. 1993a; 7:779–784. [PubMed: 8119433]

Quantock AJ, Young RD. Development of the corneal stroma, and the collagen-proteoglycan associations that help define its structure and function. Dev Dyn. 2008; 237:2607–2621. [PubMed: 18521942]

Radner W, Zehetmayer M, Aufreiter R, Mallinger R. Interlacing and cross-angle distribution of collagen lamellae in the human cornea. Cornea. 1998; 17:537–543. [PubMed: 9756449]

Rao RA, Mehta MR, Toussaint KC Jr. Fourier transform-second-harmonic generation imaging of biological tissues. Optics express. 2009; 17:14534–14542. [PubMed: 19687932]

Rawe IM, Leonard DW, Meek KM, Zabel RW. X-ray diffraction and transmission electron microscopy of Morquio syndrome type A cornea: a structural analysis. Cornea. 1997; 16:369–376. [PubMed: 9143815]

Rawe IM, Meek KM, Leonard DW, Takahashi T, Cintron C. Structure of corneal scar tissue: an X-ray diffraction study. Biophys J. 1994; 67:1743–1768. [PubMed: 7819506]

Ruberti JW, Curcio CA, Millican CL, Menco BP, Huang JD, Johnson M. Quick-freeze deep-etch visualization of age related lipid accumulation in Bruch's membrane. Invest Ophthalmol Vis Sci. 2003; 44:1753–1759. [PubMed: 12657618]

Sabatini DD, Bensch K, Barnett RJ. Cytochemistry and electron microscopy. The preservation of cellular ultrastructure and enzymatic activity by aldehyde fixation. J Cell Biol. 1963; 17:19–58. [PubMed: 13975866]

Sayers Z, Whitburn SB, Koch MHJ, Meek KM, Elliott GF. Synchrotron X-ray diffraction study of corneal stroma. J Mol Biol. 1982; 160:593–607. [PubMed: 7175938]

Scott JE. Proteodermatan and proteokeratan sulphate (decorin/lumican/fibromodulin) proteins are horseshoe shaped. Implications for their interactions with collagen. Biochem. 1996; 35:8795–8799. [PubMed: 8688414]

Scott JE, Haigh M. Small'-proteoglycan:collagen interactions: keratan sulphate proteoglycan associates with rabbit corneal collagen fibrils at the 'a' and 'c' bands. Biosci Rep. 1985; 5:765–774. [PubMed: 2935202]

Scott JE, Haigh M. Keratan sulphate and the ultrastructure of cornea and cartilage: a "stand-in" for chondtoitin sulphate in conditions of oxygen lack? J Anat. 1988; 158:95–108. [PubMed: 2976065]

Scott JE, Orford CR, Hughes EW. Proteoglycan-collagen arrangements in developing rat tail tendon. An electron microscopical and biochemical investigation. Biochem J. 1981; 195:573–581. [PubMed: 6459082]

Sheppard J, Hayes S, Boote C, Votruba M, Meek KM. Changes in corneal collagen architecture during mouse postnatal development. Invest Ophthalmol Vis Sci. 2010; 51:2936–2942. [PubMed: 20089872]

Shu X, Lev-Ram V, Deerinck TJ, Qi Y, Ramko EB, Davidson MW, Jin Y, Ellisman MH, Tsien RY. A genetically encoded tag for correlated light and electron microscopy of intact cells, tissues, and organisms. PLoS Biol. 2011; 9:e1001041. [PubMed: 21483721]

Siegler V, Quantock AJ. Two-stage compaction of the secondary avian cornea during development. Exp Eye Res. 2002; 74:427–431. [PubMed: 12014925]

Smolek MK, Klyce SD. Is keratoconus a true ectasia? An evaluation of corneal surface area. Archives of ophthalmology. 2000; 118:1179–1186. [PubMed: 10980762]

Stoller P, Reiser KM, Celliers PM, Rubenchik AM. Polarization-modulated second harmonic generation in collagen. Biophysical journal. 2002; 82:3330–3342. [PubMed: 12023255]

Studer H, Larrea X, Riedwyl H, Buchler P. Biomechanical model of human cornea based on stromal microstructure. J Biomechanics. 2010; 43:836–842.

Svensson L, Aszodi A, Reinholt FP, Fassler R, Heinegard D, Oldberg A. Fibromodulin-null mice have abnormal collagen fibrils, tissue organization, and altered lumican deposition in tendon. The Journal of biological chemistry. 1999; 274:9636–9647. [PubMed: 10092650]

Tan HY, Chang YL, Lo W, Hsueh CM, Chen WL, Ghazaryan AA, Hu PS, Young TH, Chen SJ, Dong CY. Characterizing the morphologic changes in collagen crosslinked-treated corneas by Fourier transform-second harmonic generation imaging. J Cataract Refract Surg. 2013; 39:779–788. [PubMed: 23608570]

Tan HY, Sun Y, Lo W, Lin SJ, Hsiao CH, Chen YF, Huang SC, Lin WC, Jee SH, Yu HS, Dong CY. Multiphoton fluorescence and second harmonic generation imaging of the structural alterations in keratoconus ex vivo. Invest Ophthalmol Vis Sci. 2006; 47:5251–5259. [PubMed: 17122110]

Tan HY, Sun Y, Lo W, Teng SW, Wu RJ, Jee SH, Lin WC, Hsiao CH, Lin HC, Chen YF, Ma DH, Huang SC, Lin SJ, Dong CY. Multiphoton fluorescence and second harmonic generation microscopy for imaging infectious keratitis. Journal of biomedical optics. 2007; 12:024013. [PubMed: 17477728]

Tan HY, Teng SW, Lo W, Lin WC, Lin SJ, Jee SH, Dong CY. Characterizing the thermally induced structural changes to intact porcine eye, part 1: second harmonic generation imaging of cornea stroma. Journal of biomedical optics. 2005; 10:054019. [PubMed: 16292979]

Tasheva ES, Koester A, Paulsen AQ, Garrett AS, Boyle DL, Davidson HJ, Song M, Fox N, Conrad GW. Mimecan/osteoglycin-deficient mice have collagen fibril abnormalities. Mol Vis. 2002; 31:407–415. [PubMed: 12432342]

Tektas OY, Lütjen-Drecoll E. Structural changes in the trabecular meshwork in different kinds of glaucoma. Exp Eye Res. 2009; 88:769–75. [PubMed: 19114037]

Teng SW, Tan HY, Peng JL, Lin HH, Kim KH, Lo W, Sun Y, Lin WC, Lin SJ, Jee SH, So PT, Dong CY. Multiphoton autofluorescence and second-harmonic generation imaging of the ex vivo porcine eye. Invest Ophthalmol Vis Sci. 2006; 47:1216–1224. [PubMed: 16505061]

Teng SW, Tan HY, Sun Y, Lin SJ, Lo W, Hsueh CM, Hsiao CH, Lin WC, Huang SC, Dong CY. Multiphoton fluorescence and second-harmonic-generation microscopy for imaging structural alterations in corneal scar tissue in penetrating full-thickness wound. Archives of ophthalmology. 2007; 125:977–978. [PubMed: 17620585]

Trelstad, RL.; Birk, DE. Collagen fibril assembly at the surface of polarized cells. In: Trelstad, RL., editor. The role of extracellular matrix in development. Alan R. Liss, Inc.; New York: 1984. p. 513-543.

Tuer AE, Akens MK, Krouglov S, Sandkuijl D, Wilson BC, Whyne CM, Barzda V. Hierarchical model of fibrillar collagen organization for interpreting the second-order susceptibility tensors in biological tissue. Biophysical journal. 2012; 103:2093–2105. [PubMed: 23200043]

Vanhecke D, Graber W, Studer D. Close-to-native ultrastructural preservation by high pressure freezing. Methods Cell Biol. 2008; 88:151–164. [PubMed: 18617033]

Wall RS, Elliott GF, Gyi TJ, Meek KM, Branford-White CJ. Bovine corneal stroma contains a structural glycoprotein located in the gap region of the collagen fibrils. Biosci Rep. 1988; 8:77–83. [PubMed: 3395675]

Wang BG, Eitner A, Lindenau J, Halbhuber KJ. High-resolution two-photon excitation microscopy of ocular tissues in porcine eye. Lasers in surgery and medicine. 2008; 40:247–256. [PubMed: 18412222]

Wang BG, Halbhuber KJ. Corneal multiphoton microscopy and intratissue optical nanosurgery by nanojoule femtosecond near-infrared pulsed lasers. Annals of anatomy = Anatomischer Anzeiger : official organ of the Anatomische Gesellschaft. 2006; 188:395–409. [PubMed: 16999201]

Ward NP, Scott JE, Coster L. Dermatan sulphate proteoglycans from sclera examined by rotary shadowing and electron microscopy. Biochem J. 1987; 242:761–766. [PubMed: 3593274]

Williams RM, Zipfel WR, Webb WW. Interpreting second-harmonic generation images of collagen I fibrils. Biophysical journal. 2005; 88:1377–1386. [PubMed: 15533922]

Winkler M, Chai D, Kriling S, Nien CJ, Brown DJ, Jester B, Juhasz T, Jester JV. Nonlinear optical macroscopic assessment of 3-D corneal collagen organization and axial biomechanics. Invest Ophthalmol Vis Sci. 2011; 52:8818–8827. [PubMed: 22003117]

Winkler M, Jester BE, Nien-Shy C, Chai D, Brown DJ, Jester JV. High resolution macroscopy (HRMac) of the eye using non-linear optical imaging. Proceeding of SPIE. 2010a; 7589:758906, 758901–758907.

Winkler M, Jester BE, Nien-Shy C, Massei S, Minckler DS, Jester JV, Brown DJ. High resolution three-dimensional reconstruction of the collagenous matrix of the human optic nerve head. Brain research bulletin. 2010b; 81:339–348. [PubMed: 19524027]

Winkler M, Shoa G, Xie Y, Petsche SJ, Pinsky PM, Juhasz T, Brown DJ, Jester JV. Three-dimensional distribution of transverse collagen fibers in the anterior human corneal stroma. Invest Ophthalmol Vis Sci. 2013; 54:7293–7301. [PubMed: 24114547]

Worthington CR, Inouye H. X-ray diffraction study of the cornea. Int J Biol Macromol. 1985; 7:2–8.

Wu Q, Yeh AT. Rabbit cornea microstructure response to changes in intraocular pressure visualized by using nonlinear optical microscopy. Cornea. 2008; 27:202–208. [PubMed: 18216577]

Yeh AT, Nassif N, Zoumi A, Tromberg BJ. Selective corneal imaging using combined second-harmonic generation and two-photon excited fluorescence. Optics letters. 2002; 27:2082–2084. [PubMed: 18033448]

Young RD. The ultrastructural organisation of proteoglycans and collagen in human and rabbit scleral matrix. J Cell Sci. 1985; 74:95–104. [PubMed: 4030913]

Young RD, Quantock AJ, Sotozono C, Koizumi N, Kinoshita S. Sulphation patterns of keratan sulphate proteoglycan in sclerocornea resemble cornea rather than sclera. Br J Ophthalmol. 2006; 90:391–393. [PubMed: 16488970]

Young RD, Gealy EC, Liles M, Caterson B, Ralphs JR, Quantock AJ. Keratan sulfate glycosaminoglycan and the association with collagen fibrils in rudimentary lamellae in the developing avian cornea. Invest Ophthalmol Vis Sci. 2007; 48:3083–3088. [PubMed: 17591877]

Young RD, Liskova P, Pinali P, Palka BP, Palos M, Jirsova K, Hrdlickova E, Tesarova M, Elleder M, Zeman J, Meek KM, Knupp C, Quantock AJ. Large proteoglycan complexes and disturbed

collagen architecture in the corneal extracellular matrix of mucopolysaccharidosis Type VII (Sly Syndrome). Invest Opthalmol Vis Sci. 2011; 52:6720–6728.

Young RD, Knupp C, Pinali C, Png KM, Ralphs JR, Bushby AJ, Starborg T, Kadler KE, Quantock AJ. Three-dimensional aspects of matrix assembly by cells in the developing cornea. Proceedings of the National Academy of Sciences of the United States of America. 2014; 111:687–692. [PubMed: 24385584]

Young RD, Knupp C, Pinali C, Png KMY, Ralphs JR, Bushby AJ, Starborg T, Kadler KE, Quantock AJ. Three-dimensional aspects of matrix assembly by cells in the developing cornea. Proc Nat Acad Sci USA. 2014; 111:687–692. [PubMed: 24385584]

Young RD, Powell J, Watson PG. Ultrastructural changes in scleral proteoglycans precede destruction of the collagen fibril matrix in necrotising scleritis. Histopathology. 1988; 12:75–84. [PubMed: 3371895]

Young RD, Swamynathan SK, Boote C, Mann M, Quantock AJ, Piatigorsky J, Funderburgh JL, Meek KM. Stromal edema in klf4 conditional null mouse cornea is associated with altered collagen fibril organization and reduced proteoglycans. Invest Ophthalmol Vis Sci. 2009; 50:4155–4161. [PubMed: 19387067]

Zhang G, Chen S, Goldoni S, Calder BW, Simpson HC, Owens RT, McQuillan DJ, Young MF, Iozzo RV, Birk DE. Genetic evidence for the coordinated regulation of collagen fibrillogenesis in the cornea by decorin and biglycan. J Biol Chem. 2009; 284:8888–8897. [PubMed: 19136671]

Zhang G, Young BB, Ezura Y, Favata M, Soslowsky LJ, Chakravarti S, Birk DE. Development of tendon structure and function: regulation of collagen fibrillogenesis. J Musculoskeletal & neuronal interactions. 2005; 5:5–21.

Zipfel WR, Williams RM, Christie R, Nikitin AY, Hyman BT, Webb WW. Live tissue intrinsic emission microscopy using multiphoton-excited native fluorescence and second harmonic generation. Proc Nat Acad Sci USA. 2003; 100:7075–7080. [PubMed: 12756303]

Zoumi A, Yeh A, Tromberg BJ. Imaging cells and extracellular matrix in vivo by using second-harmonic generation and two-photon excited fluorescence. Proc Nat Acad Sci USA. 2002; 99:11014–11019. [PubMed: 12177437]

Highlights

- Methods used to characterize the hierarchical assembly of the ECM are discussed.
- 3-D analysis of ECM structure by TEM/SEM and NLO SHG microscopy are presented.
- New insights into the structural blueprint of the cornea are uncovered.

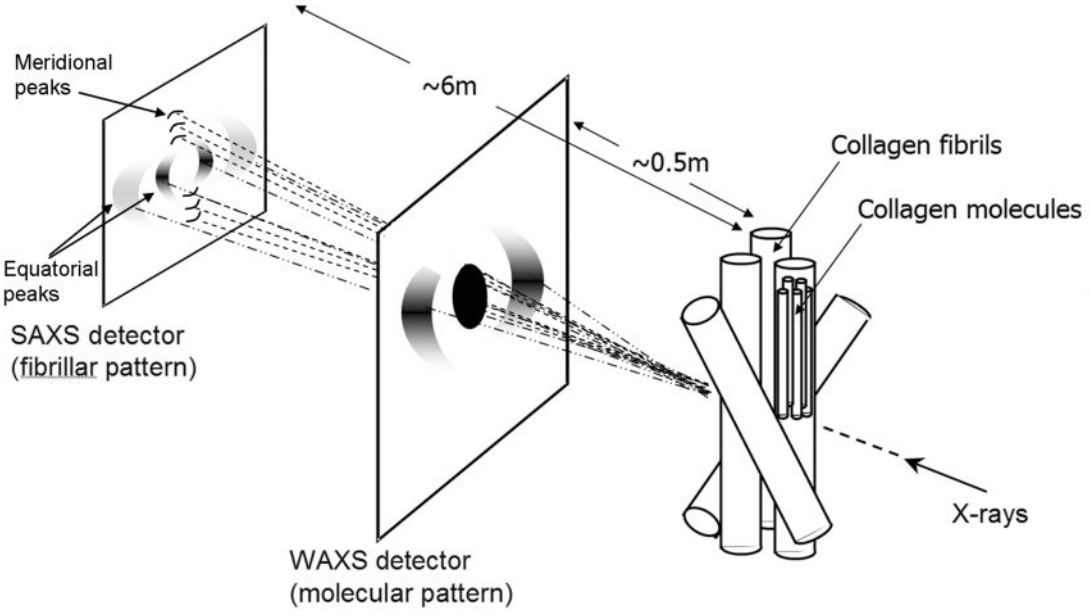

Fig. 1.

A schematic representation of small-angle X-ray scattering (SAXS) and wide-angle X-ray scattering (WAXS) from regularly spaced and uniform diameter collagen fibrils as would be found in the cornea. Small- and wide-angle scatter is produced simultaneously, and it is simply the position of the detector (or detectors) which dictates whether SAXS or WAXS patterns (or both) are recorded. In cornea, WAXS patterns, which arise from the average lateral spacing between adjacent collagen *molecules* within fibrils, provide structural information on the nanometer scale (the average intermolecular spacing in normally hydrated human cornea is about 1.6nm (Meek et al, 1991)). The equatorial portion of the SAXS patterns, on the other hand, which arise because of the regular lateral spacing of collagen *fibrils* within lamellae, provide structural information on length scales up to maybe 100nm (the average interfibrillar spacing in normally hydrated human cornea is about 65nm (Meek et al, 1991)). The meridional part of the SAXS pattern consists of a series of x-ray reflections which index on the 65nm D-periodic repeat along the axis of the corneal collagen fibrils. These can be analysed to provide conformational information about the axial electron density along the fibril, including potentially the binding locations of various collagen-associated matrix molecules.

Fig. 2.

Cuprolinic blue reveals associations of proteoglycans with collagen fibrils in the sclera of a patient with nanophthalmos. Bar = 1.5 μm

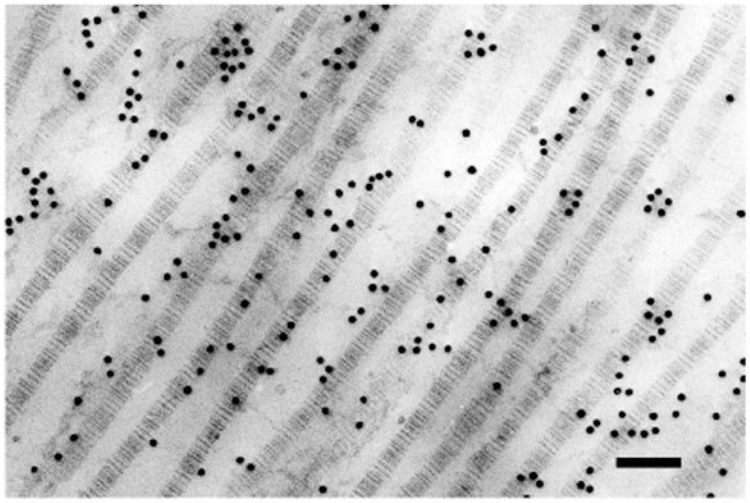

Fig. 3.

Gold particles (10 nm) which label the binding of antibody 5-D-4 along collagen fibrils in swollen bovine corneal stroma and which indicate sites of highly-sulphated keratan sulphate glycosaminoglycan. Bar = 100 nm

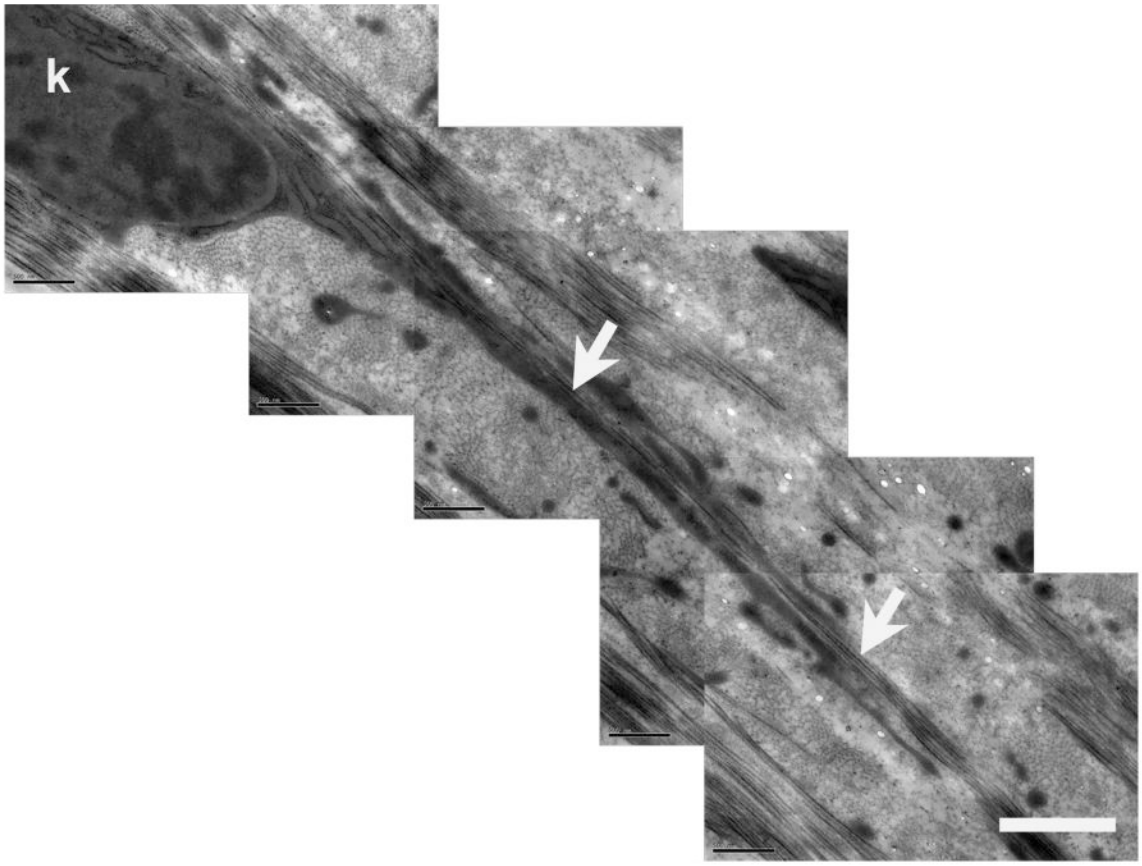

Fig. 4.

Chick cornea at day 14 of development prepared by high pressure freezing and freeze substitution. A keratocyte (k) extends a long cellular process in contact with collagen fibrils (arrows) in the extracellular matrix. Bar = 1 μm. Image courtesy of Dr Philip N. Lewis, Cardiff University.

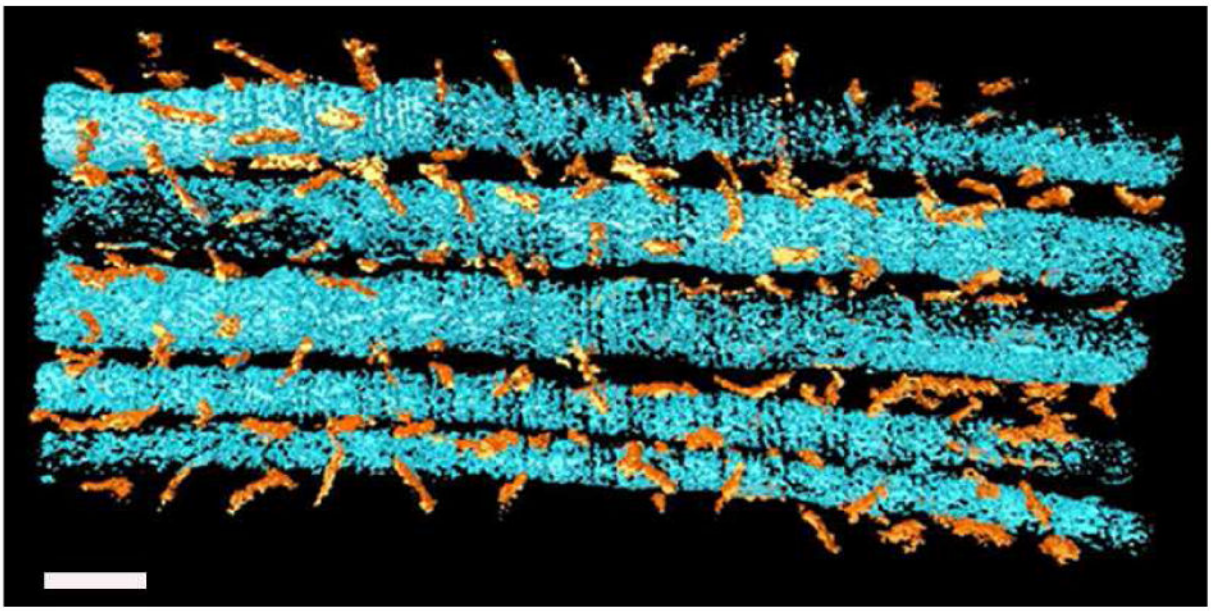

Fig. 5.

Three-dimensional reconstruction from electron tomography of anterior sclera from an 89-year-old human eye showing collagen fibrils (blue) and proteoglycans (orange). Bar = 100 nm.

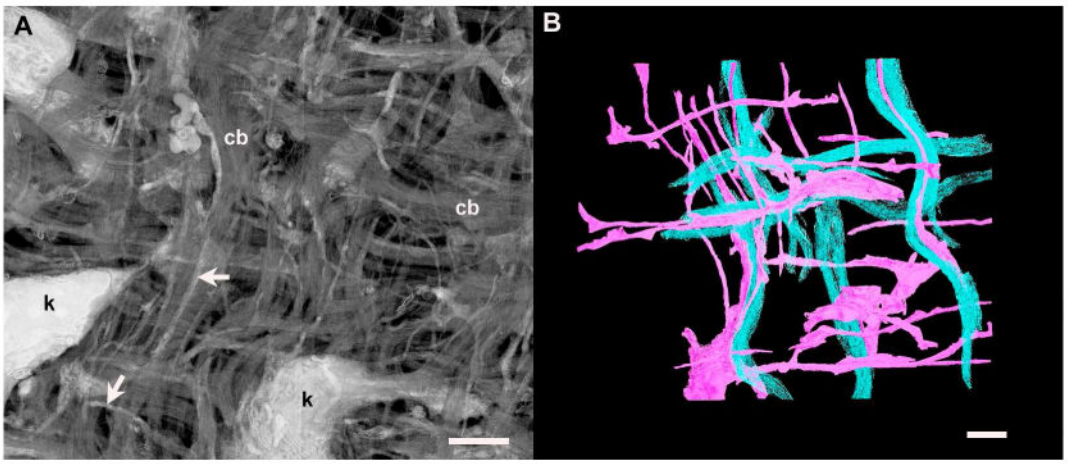

Fig. 6.

A. Developing chick cornea at 12 days of incubation: a reconstruction in ImageJ-3D viewer from 50 serial images obtained by SBF-SEM, showing keratocytes (k), with extensive processes -keratopodia (arrows), and collagen bundles (cb). Bar = 500 nm. B. Surface rendering of a three-dimensional reconstruction from 120 serial images of the same site as in A shows collagen bundles (cyan) closely accompanied by keratopodia (pink). Bar = 1 μm.

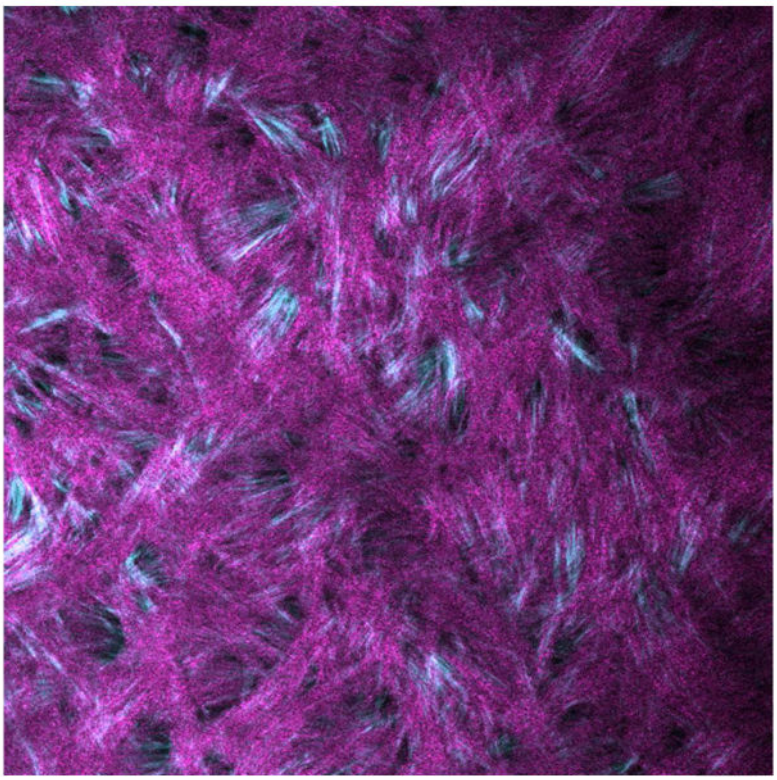

Fig. 7.

NLO SHG image of the anterior human cornea. SHG signals were detected in the forward scattered (cyan) and backscattered (magenta) direction.

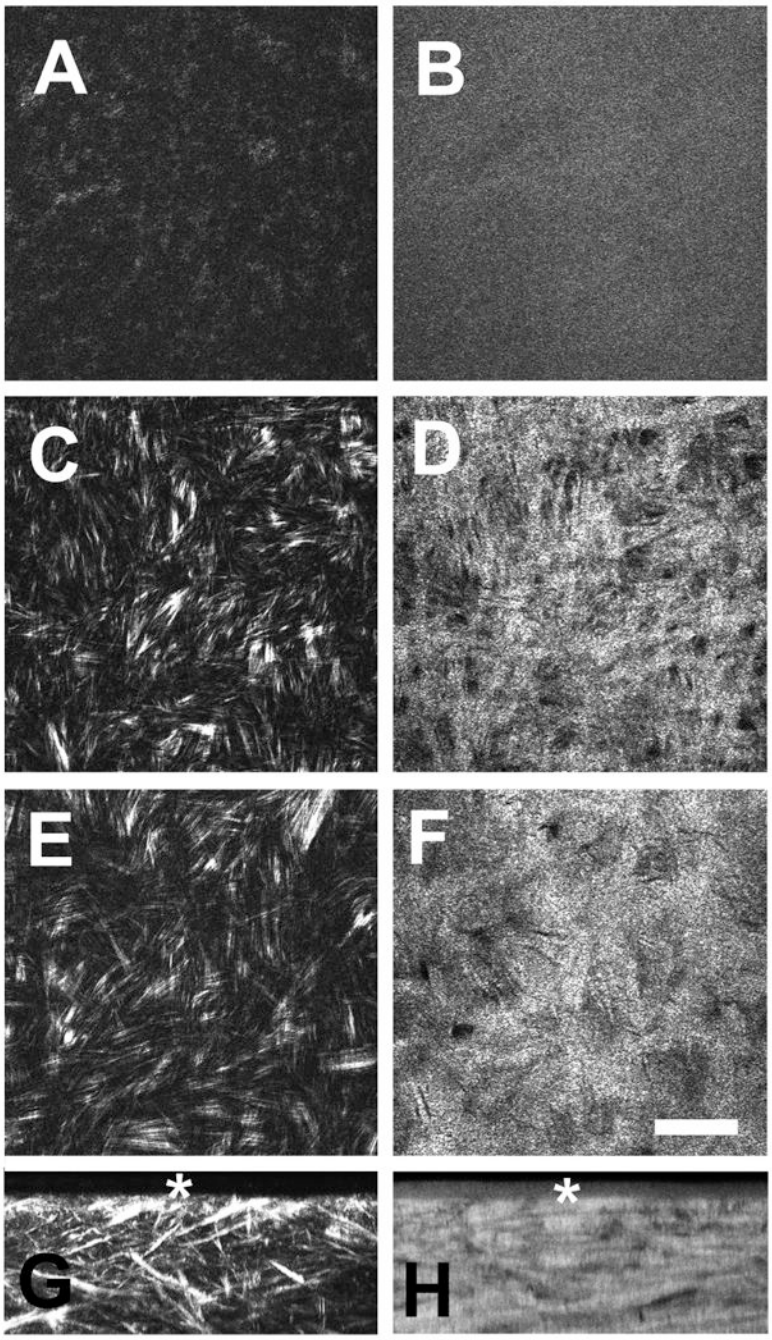

Fig. 8.

NLO SHG image from human cornea showing forward scattered (A, C, E, G) and backscattered (B, D, F, H) images taken at different depths. **A**, **B**: Anterior limiting lamina (ALL). **C**, **D**: 10 μm below A. **E**, **F**: 50 μm below A. **G**: Three-dimensional reconstruction of the data set from forward detector showing a maximum intensity projection rotated 90° in the *Y*-axis through 230 μm of anterior stroma. **H**: Asterisk = Anterior limiting lamina. Bar = 50 μm. Taken from {Morishige, 2007 #9}.

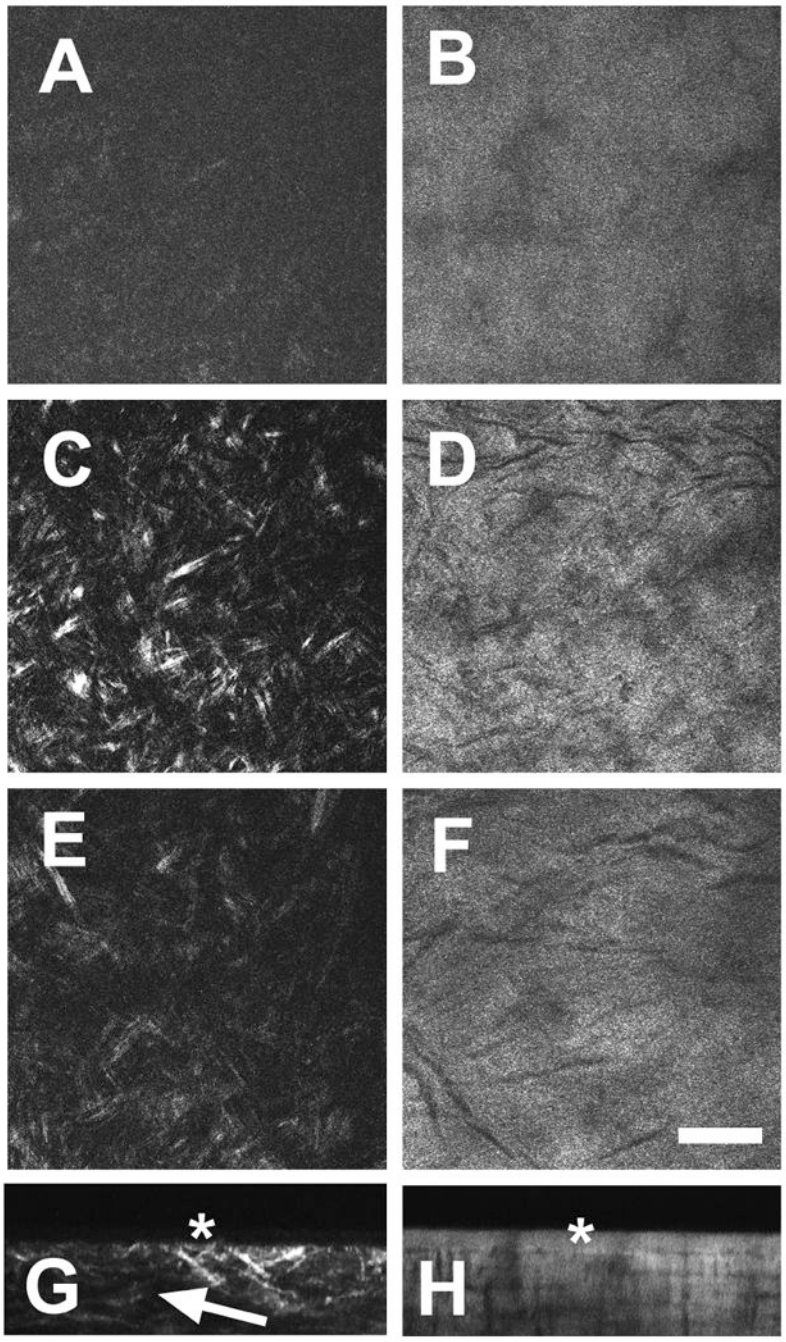

Fig. 9.

NLO SHG of keratoconus cornea showing forward scattered (A, C, E, G) and backscattered signals (B, D, F, H). **A**, **B**: Anterior limiting lamina (ALL). **C**, **D**: 10 μm below A. **E**, **F**: 50 μm below A. **G**: Three-dimensional reconstruction of forward scattered signals showing loss or shortening of lamellae inserting into the ALL (arrow) **H**: Three-dimensional reconstruction of backscattered SHG signal. Asterisk = ALL. Bar = 50 μm. Taken from {Morishige, 2007 #9}.

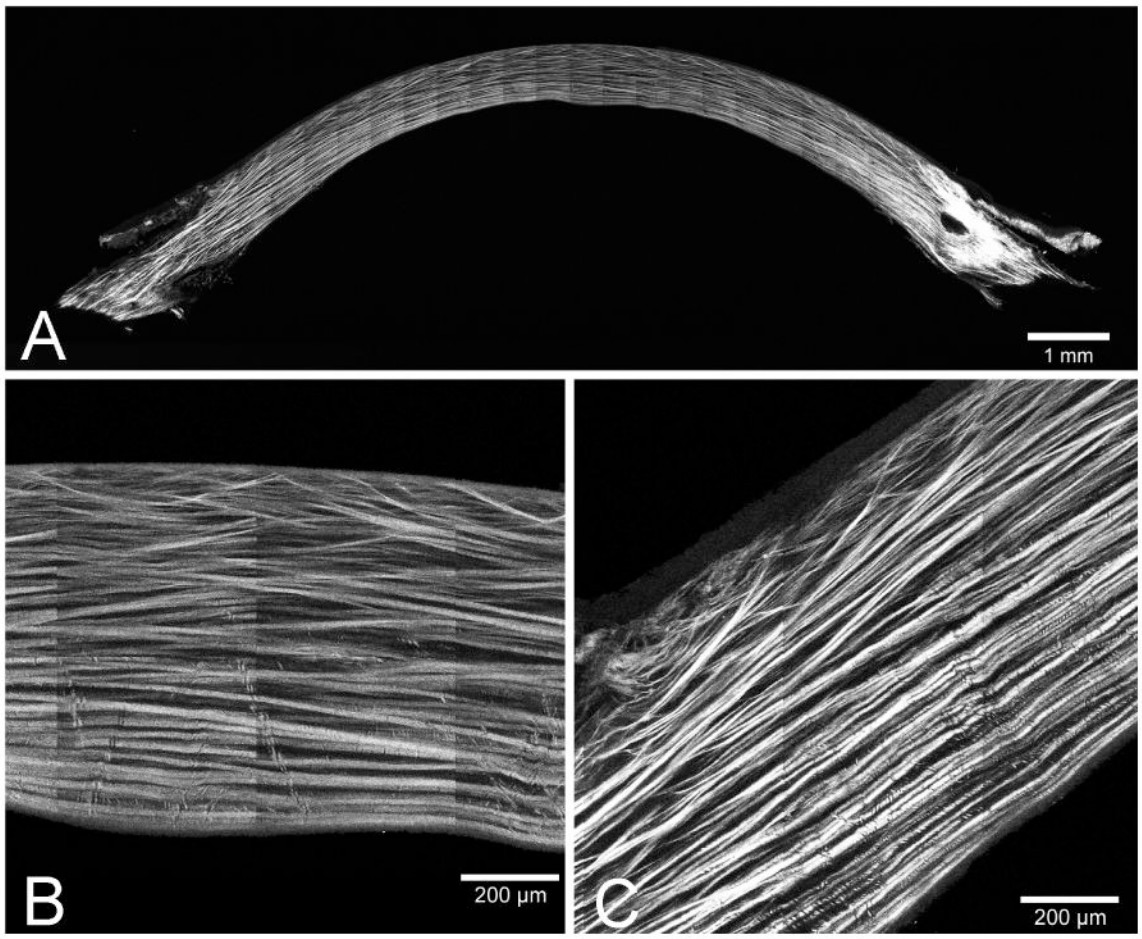

Fig. 10.

HRMac reconstruction of a human cornea. (A) Single 80 Meg pixel plane showing collagen fiber organization from superior to inferior limbus. (B) Zoomed view of the central cornea from the 80 Meg pixel plane showing insertion of anterior collagen fibers into the ALL (Bowman's layer). (C) Zoomed view of the 80 Meg pixel plane showing the collagen fiber organization at the limbus. Taken from {Jester, 2010 #16}.

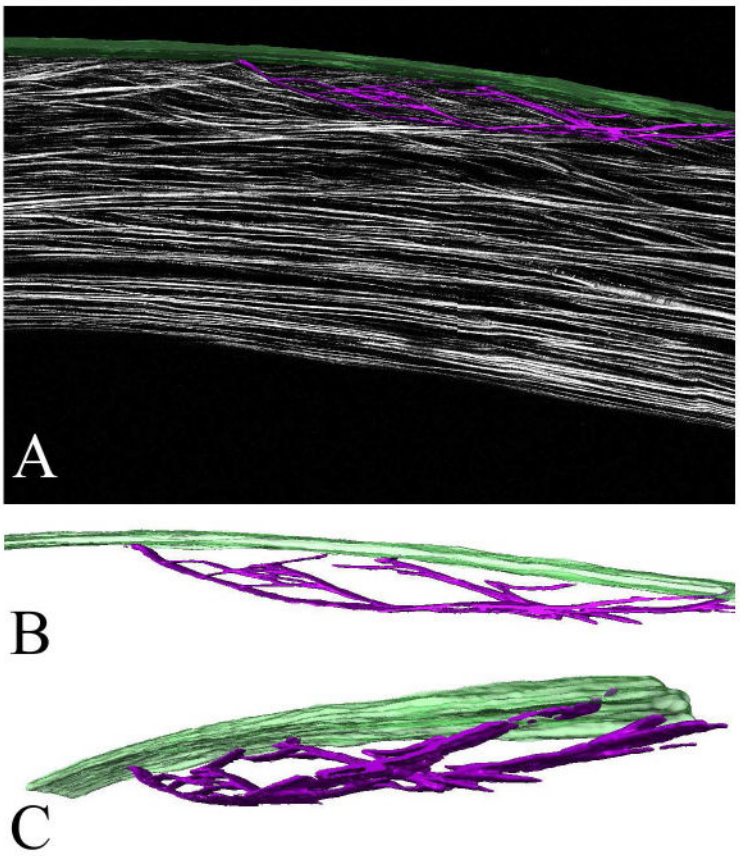

Fig. 11.

Three-dimensional reconstructed sutural lamellae in the human cornea. (A) 1 mm central corneal region from a HRMac corneal cross-section after segmentation in Amira. Bowman's layer is rendered in green, the surtural lamellae are purple. (B) and (C) show the extracted sutural lamellae rendering in two different rotations. These images can be panned, zoomed and rotated at will. Taken from Winkler et al, High resolution macroscopy (HRMac) of the eye using non-linear optical imaging. Taken from {Winkler, 2010 #79}.

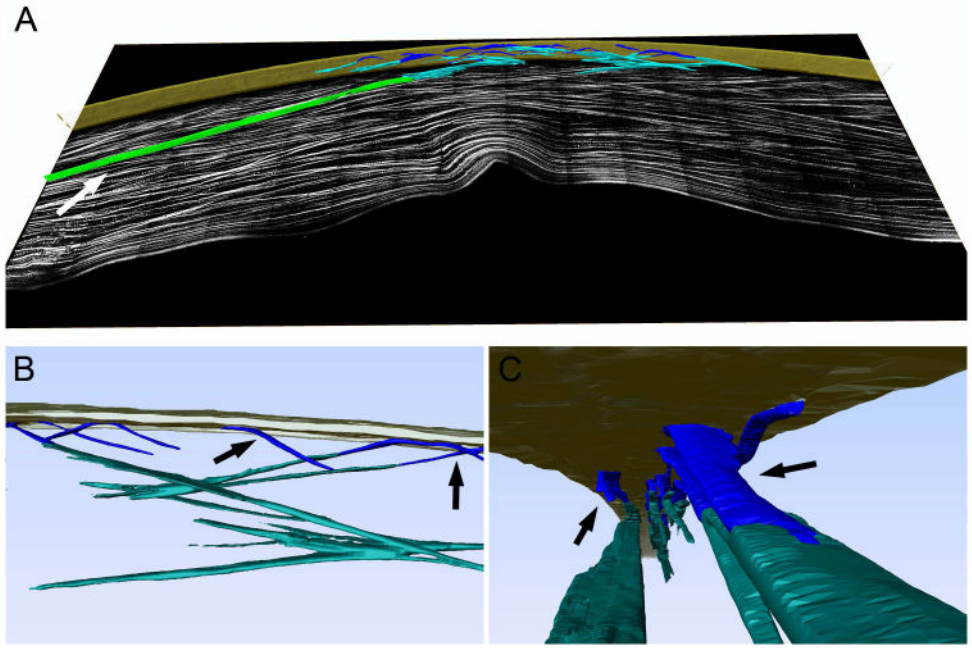

Fig. 12.

Three-dimensional reconstruction of “bow-spring” fibers (blue), anchoring fibers inserting from the limbus (green) and the highly intertwined anterior fiber meshwork (teal) near the anterior limiting lamina ALL (gold). Taken from {Winkler, 2011 #14}.

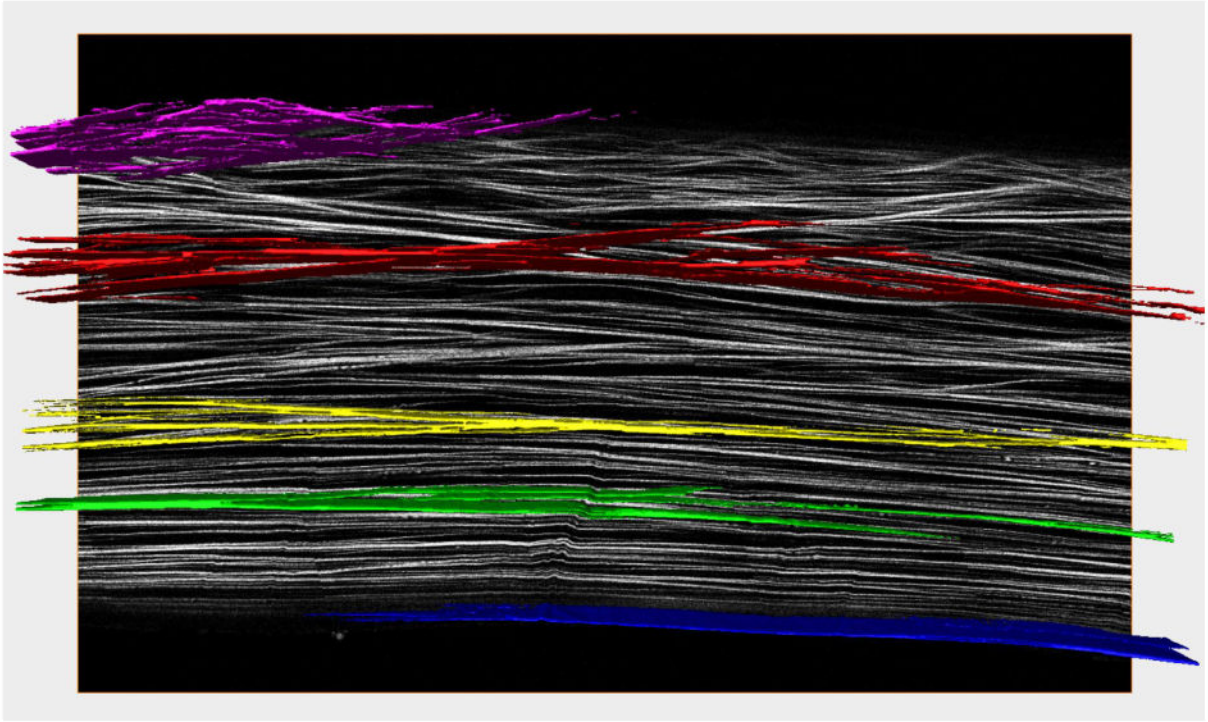

Fig. 13.

Three-dimensional surface renderings of selected collagen fibers from the anterior (purple) to the posterior (blue) central cornea. Note that branching and anastomosing of fibers drops from anterior to posterior cornea.